

# Embedded, Doubly Periodic Minimal Surfaces

Wayne Rossman, Edward C. Thayer, and Meinhard Wohlgemuth

## CONTENTS

1. Introduction
  2. Overview of the Construction
  3. Background Results Needed for the Construction
  4. The Examples  $M_k$
  5. The Examples  $M_k^+$
  6. The Examples  $M_k^-$
  7. The Examples  $M_{2k+1}^-$
  8. The Examples  $M_{2k+1}^{++}$
  9. The Examples  $M_k^{+-}$
- Appendix: A Proof of Lemma 4.1
- Acknowledgements
- References

Thayer was supported by the National Science Foundation under grants DMS-9011083 and DMS-9312087 and by the U.S. Department of Energy under grant DE-FG02-86ER25015 of the Applied Mathematical Science subprogram of the Office of Energy Research. Wohlgemuth was supported by SFB 256 at University of Bonn and the Alexander von Humboldt-Stiftung.

---

We consider the question of existence of embedded doubly periodic minimal surfaces in  $\mathbb{R}^3$  with Scherk-type ends, surfaces that topologically are Scherk's doubly periodic surface with handles added in various ways. We extend the existence results of H. Karcher and F. Wei to more cases, and we find other cases where existence does not hold.

---

## 1. INTRODUCTION

H. Karcher [1991] proved the existence of the first complete, embedded, doubly periodic minimal surface to be found since H. Scherk's classical example, which dates from 1835. We denote Karcher's surface by  $M_1$  (see Figure 1, left). Following this discovery, Wei [1992] constructed an embedded, doubly periodic surface of genus two by adding a handle to  $M_1$  (Figure 1, center). We describe a new embedded, genus two surface that results from adding a different type of handle to  $M_1$  (Figure 1, right), and outline the differences between these two genus two surfaces. In addition, we construct three collections of new, embedded surfaces of genus three that result from adding either two handles of the same type (see Figure 2) or two handles of different type (see Figure 3).

Using a technique discovered by Karcher and Polthier [1993] to reduce the number of periods to be considered, we are able to add ends to the fundamental piece of each surface presented without increasing the dimension of the period problems, thereby producing countably many different families of new, embedded examples for each of the handle types shown in Figures 1 and 2.

The existence proofs for the genus two surfaces require solving one-dimensional period problems, and the existence proofs for the genus three surfaces require solving either one-dimensional or two-dimensional period problems, depending on the types of handles we choose. When the period problem is one-

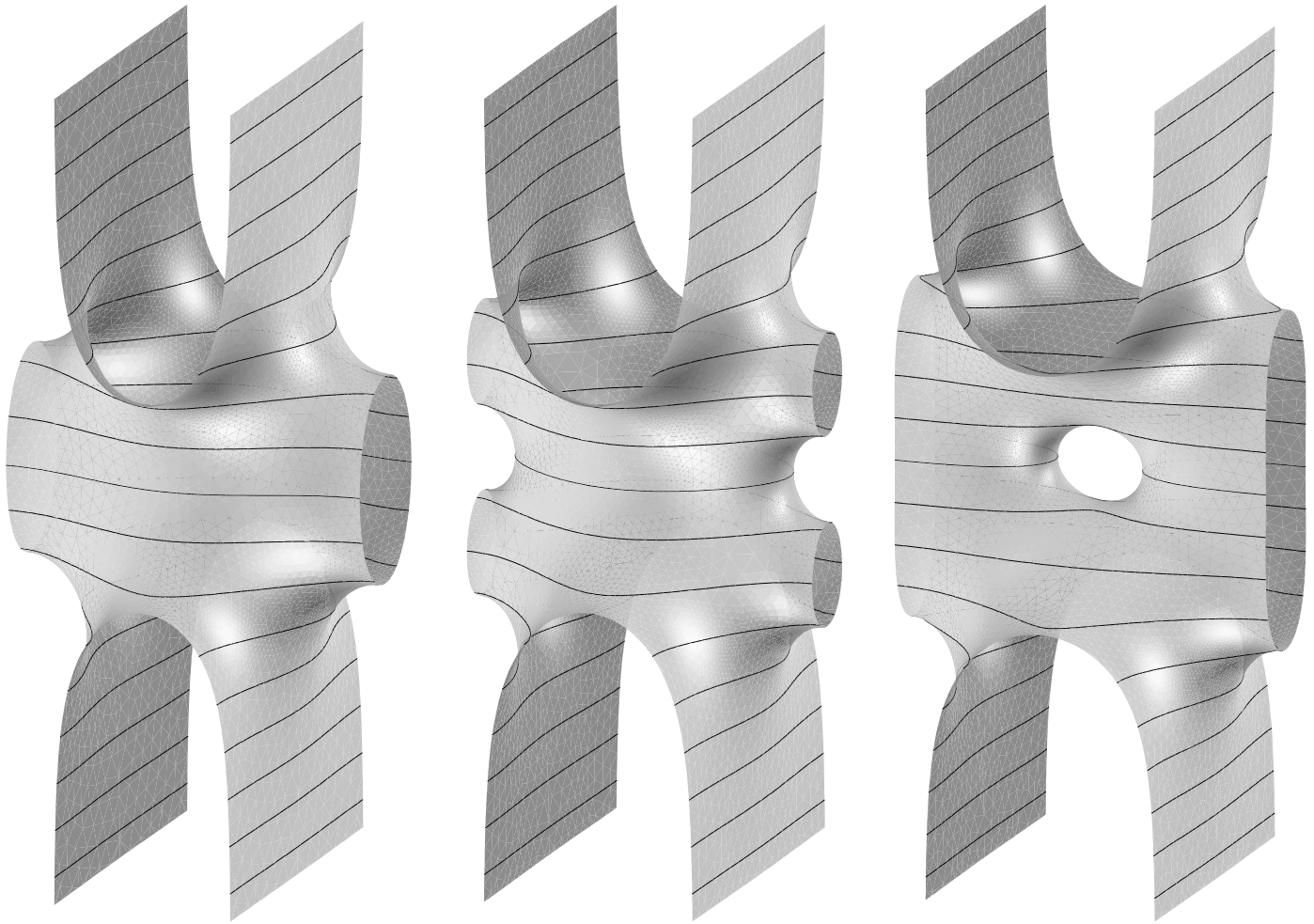


**FIGURE 1.** Fundamental pieces of Karcher's surface  $M_1$  (left), Wei's surface  $M_1^-$  (center), and the surface  $M_1^+$ .

dimensional (as for the surfaces in Figures 1 and 2), we use the intermediate value theorem to solve it. When it is two-dimensional (as for the surfaces in Figure 3), we achieve a solution by using a mapping degree argument, a kind of generalization of the intermediate value theorem.

We find that in the two cases of genus three surfaces with four ends and handles of the same type the period problems have no solution. In these exceptional cases we demonstrate a natural geometric obstruction to existence, an obstruction that disappears when more ends are added to the surfaces.

## 2. OVERVIEW OF THE CONSTRUCTION

Karcher's original surfaces  $M_1$  are highly symmetric; they have three mutually perpendicular planes of symmetry and contain four vertical straight lines

(Figures 1, left and 5, left). The three planes divide the surface into eight pieces. Each piece is bounded by planar geodesic curves, and has one end. Since all the surfaces we will discuss here share these planar symmetries we will focus on one eighth of these surfaces and draw sketches of this portion only.

The first modification of  $M_1$  was made by F. Wei [1992], who constructed a one-parameter family of genus two examples  $M_1^-$  by adding a single handle over one of the two saddle points of  $M_1$  (see Figures 1, center and 5, center). Recently it was discovered by Karcher and Polthier [1993] (and the second author independently) that another modification of  $M_1$  was possible. This new surface  $M_1^+$  results from adding a handle to  $M_1$  in a different direction, thereby producing another doubly periodic, embedded minimal surface of genus two. See Figures 1, right and 5, right.

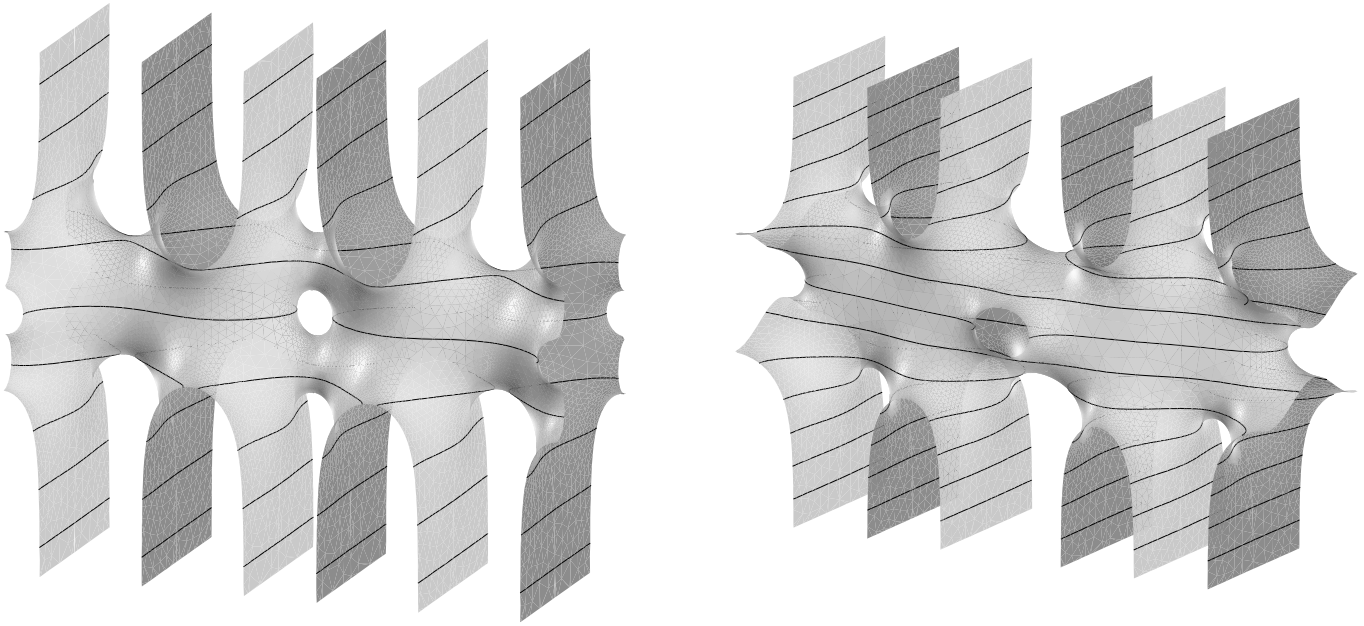


FIGURE 2. Fundamental pieces of  $M_3^{--}$  and  $M_3^{++}$ .

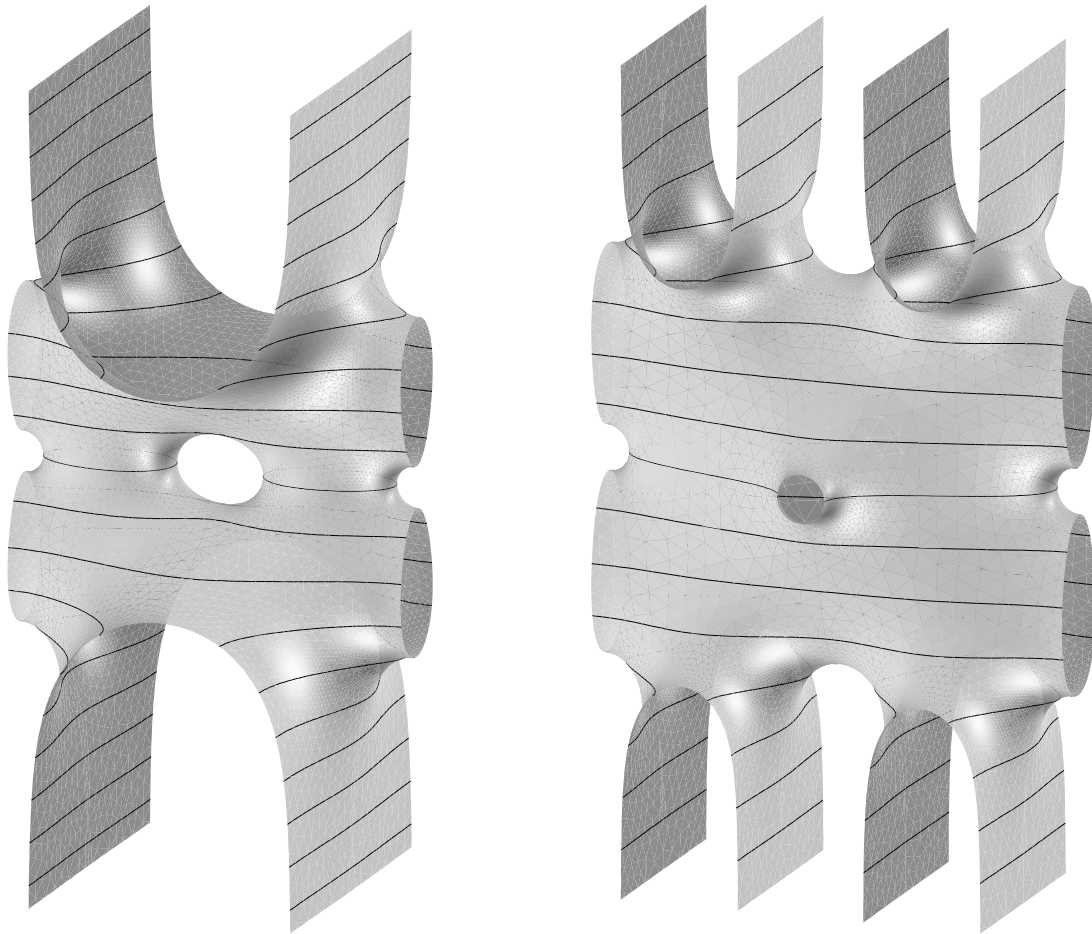


FIGURE 3. Fundamental pieces of  $M_1^{+-}$  (left) and  $M_2^{+-}$  (right).

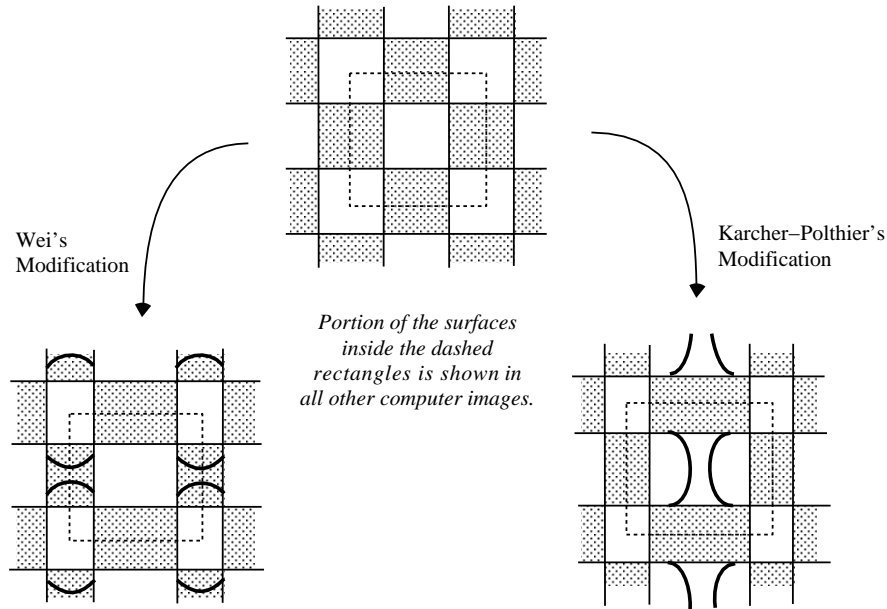


FIGURE 4.  $M_1$ ,  $M_1^-$ , and  $M_1^+$  projected onto the  $x_1$ - $x_2$  plane.

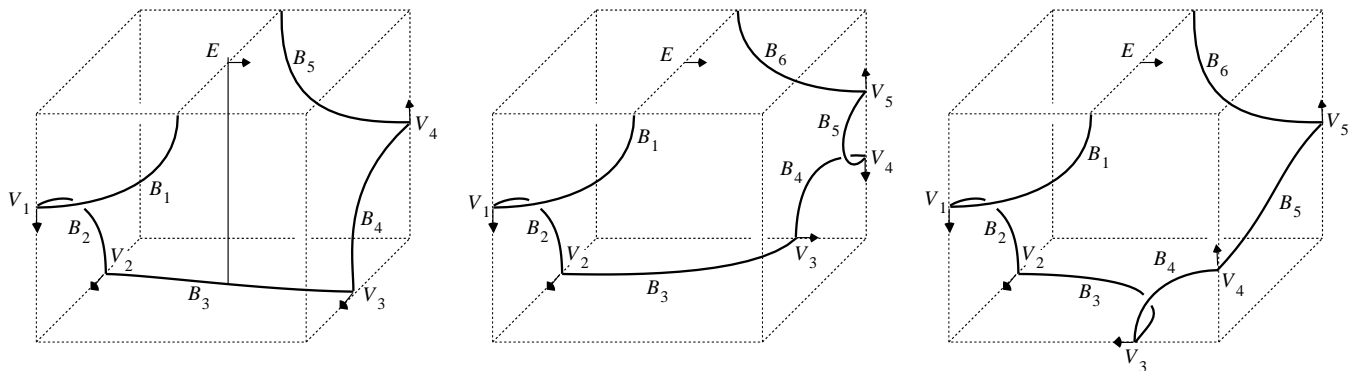


FIGURE 5. Sketches of one eighth of  $M_1$ (left),  $M_1^-$ (center), and  $M_1^+$ (right).

**Remark on Notation.** In order to distinguish the two genus two surfaces, we view  $M_1$  from above, imagining that  $M_1$  projects into the black squares of an infinite, black and white checkerboard pattern, with the vertical straight lines projecting onto the corners of these squares (see Figure 4). From this perspective, the handles added by Wei project into the black regions while the new handles project into the white ones. In both cases, the additional handles modify the checker board pattern into a tiling made up of rectangular regions as is indicated in Figure 4. We denote the handles over the black squares with a superscript ‘-’, and those over the white squares with a superscript ‘+’. Hence, in this notation, Wei’s genus two surface is referred to as  $M_1^-$ , and the new surface discussed in Section 5 is  $M_1^+$ . (Each sur-

face discussed in this paper lies in a one-parameter family of embedded surfaces. Since we are interested in the topological qualities of these surfaces, our notation throughout the paper will not reflect the specific surface in the family. The subscript indexes the number of ends on each eighth of the surface.)

Both  $M_1^+$  and  $M_1^-$  have smaller symmetry groups than Karcher’s original surface; in particular, the vertical straight lines of  $M_1$  are eliminated. The question “Is it possible to add handles to  $M_1$  and preserve the original symmetries?” is a natural one. We might, for example, want to add either a ‘+’ or a ‘-’ type handle and preserve the vertical straight lines. Rotation about these lines (see Theorem 3.1) places another handle over the other saddle point

of  $M_1$ . This would result in a genus three surface with four Scherk ends. It is easy to imagine such a surface for either type of handle. Indeed, the suggested conjugate contour of one eighth of either surface supports a Plateau solution that is a Jenkins–Serrin graph [Jenkins and Serrin 1966]. So a minimal surface with boundary exists with the desired shape, but we only know that certain bounding planar curves lie in parallel planes. We then must solve the one-dimensional period problem or, equivalently, show that the parallel planes coincide. We will prove that neither of these period problems are solvable, and we do so by finding natural obstructions on the corresponding conjugate surfaces. Understanding these obstructions, we realize it is possible to overcome them by adding more ends to each surface. Because of the desired symmetries, each eighth of these surfaces must have an odd number of ends. Indexing by this number, we show the period problems are never solved on  $M_1^{--}$  and  $M_1^{++}$ , and that for  $k \geq 1$  the period problems associated to  $M_{2k+1}^{--}$  and  $M_{2k+1}^{++}$  are solvable. The superscript indicates the types of handles added to  $M_1$ . See Figure 2.

With the addition of each new end, there is a new associated period. In Section 4, we describe a technique found by Karcher and Polthier [1993] that shows that one may simultaneously solve these end periods. Specifically, they observed that a certain simple restriction on the conjugate contours ensures these end periods are all zero. Moreover, this restriction leaves an ample number of parameters free to allow us to adjust the other periods associated with the new handles.

Instead of adding two handles of the same type to  $M_1$ , we may also consider surfaces which have two handles of different types. This produces a family of genus three surfaces that no longer have the straight line symmetries of  $M_1$ . Without this additional symmetry, the period problem resulting from the new handles is two-dimensional. The third author’s experience with two-dimensional period problems [Wohlgemuth 1997] suggested that these period problems may be solvable. We prove in Section 9 that  $M_1^{+-}$  with four Scherk-type ends exists. Generalizing the examples  $M_1^{+-}$  to have  $4k$  Scherk-type ends for  $k \geq 2$ , numerical evidence suggests the existence of  $M_k^{+-}$  for  $k \geq 2$  (see Figure 3).

### 3. BACKGROUND RESULTS NEEDED FOR THE CONSTRUCTION

We consider only connected and properly immersed minimal surfaces. To establish notation we state the following description of the Weierstrass Representation.

**Theorem and Notation (Weierstrass–Representation).** *Let  $M$  be a minimal surface in  $\mathbb{R}^3$  and  $R$  the underlying Riemann surface of  $M$ . Then  $M$  can be expressed, up to translations, in terms of a meromorphic function  $g$  on  $R$ , the so-called Gauss map (since  $g$  will be stereographic projection of the oriented normal vector of  $M$ ), and a holomorphic differential  $\eta$  on  $R$  by*

$$F(p) = \operatorname{Re} \int_{p_0}^p (\varphi_1, \varphi_2, \varphi_3), \tag{3-1}$$

where  $p_0 \in R$  is fixed and

$$(\varphi_1, \varphi_2, \varphi_3) = \left( \left( \frac{1}{g} - g \right) \eta, i \left( \frac{1}{g} + g \right) \eta, 2\eta \right). \tag{3-2}$$

Conversely, let  $R$  be a Riemann surface,  $g$  a meromorphic function on  $R$ , and  $\eta$  a holomorphic differential on  $R$ . Then the two preceding equations define a conformal minimal immersion  $F : R \rightarrow \mathbb{R}^3$ , provided the poles and zeros of order  $l$  of  $g$  coincide with the zeros of order  $l$  of  $\eta$ , and  $(\varphi_1, \varphi_2, \varphi_3)$  has no real periods, that is,

$$\operatorname{Period}_{(\varphi_1, \varphi_2, \varphi_3)}(\gamma) = \int_{\gamma} (\varphi_1, \varphi_2, \varphi_3) \in i\mathbb{R} \tag{3-3}$$

for all closed curves  $\gamma$  on  $R$ .

We call  $(R, g, \eta)$  the *Weierstrass data* of the minimal surface  $M$ . Denoting the universal cover of  $R$  by  $\tilde{R}$ , the minimal immersion  $F^* : \tilde{R} \rightarrow \mathbb{R}^3$  with the Weierstrass data  $(R, g, i\eta)$  is called the *conjugate surface* to  $M$ , and is denoted by  $M^*$ . It is known that any curve of  $R$  which is mapped by  $F$  to a nonstraight planar geodesic of  $M$  is mapped by  $F^*$  to a straight line in  $M^*$ . Furthermore, since the Gauss map  $g$  and the first fundamental form are the same for both  $M$  and  $M^*$ , it follows that the planar geodesic in  $M$  will lie in a plane perpendicular to the corresponding line in  $M^*$  and that the planar geodesic in  $M$  will have the same length as the line in  $M^*$ . We will use these properties extensively. The following known results are also central to the arguments we will be making.

**Theorem 3.1 (Schwarz reflection principle).** *Suppose a minimal surface  $M \subset \mathbb{R}^3$  contains in its boundary a curve  $\mathcal{C}$  that is either a straight line or a nonstraight planar geodesic. Then  $M$  can be extended smoothly across  $\mathcal{C}$  by respectively rotation about  $\mathcal{C}$  or reflection through the plane containing  $\mathcal{C}$ .*

**Theorem 3.2** [Dierkes et al. 1992]. *If an embedded minimal surface  $F : B \rightarrow \mathbb{R}^3$ ,  $B = \{w \in \mathbb{C} : |w| < 1\}$  can be written as a graph over a convex domain in a plane, then the conjugate surface  $F^* : B \rightarrow \mathbb{R}^3$  is also a graph over a domain in the same plane.*

**Theorem 3.3** [Jenkins and Serrin 1966]. *Let  $D$  be a bounded convex domain such that  $\partial D$  contains two sets of finite numbers of open straight segments  $\{A_i\}, \{B_j\}$  with the property that no two segments  $A_i$  and no two segments  $B_j$  have a common endpoint. Let the remaining portion of  $\partial D$  consist of a finite number of open arcs  $\{C_k\}$ , and of endpoints of  $A_i, B_j$ , and  $C_k$ . Let  $\mathcal{P}$  denote a simple closed polygon whose vertices are chosen from among the endpoints of the  $A_i$  and  $B_j$ . Let*

$$\alpha = \sum_{A_i \subset \mathcal{P}} \text{length } A_i,$$

$$\beta = \sum_{B_j \subset \mathcal{P}} \text{length } B_j,$$

$$\gamma = \text{length of perimeter of } \mathcal{P}.$$

*Then if  $\{C_k\} \neq \emptyset$ , there exists a solution of the minimal surface equation in  $D$  which assumes the value  $+\infty$  on each  $A_i$ ,  $-\infty$  on each  $B_j$ , and any assigned bounded continuous data on each open arc  $C_k$  if and only if*

$$2\alpha < \gamma \text{ and } 2\beta < \gamma$$

*for each polygon  $\mathcal{P}$  chosen as above. Moreover, the solution is unique when it exists.*

**Remark 3.4.** In Theorem 3.3, we allow the possibility that two different  $C_k$  have a common endpoint. We may have jump discontinuities in the boundary data at the points where two different  $C_k$  meet. It follows from the arguments in [Jenkins and Serrin 1966] that, for  $D$  as in Theorem 3.3, if  $u_1$  and  $u_2$  are two solutions of the minimal surface equation such that  $u_1 = u_2 = +\infty$  on each  $A_i$  and  $u_1 = u_2 = -\infty$  on each  $B_j$  and  $u_1 \geq u_2$  on each  $C_k$ , then  $u_1 \geq u_2$  in the interior of  $D$ .

#### 4. THE EXAMPLES $M_k$

An immediate application of Theorems 3.2 and 3.3 is to prove that one can add more ends to Kärcher’s genus one surface  $M_1$ , thereby creating the surfaces  $M_k$ .

**Theorem 4.1.** *For each  $k \geq 2$ , there exists a one-parameter family  $M_k$  of embedded, doubly periodic minimal surfaces of genus one with  $4k$  Scherk-type ends.*

*Proof.* Fix  $k$ . The conjugate boundary of one eighth of  $M_k$  is a graph over a rectangular domain with three sides at height zero and the fourth edge subdivided into  $k$  segments with heights alternating between  $+\infty$  and  $-\infty$ . Theorem 3.3 yields a Plateau solution with this boundary. Then Theorem 3.2, together with Theorem 3.1 and the maximum principle, gives the embedded surfaces  $M_k$  from these solutions. The period problems associated to the ends, which equal the residues at the end punctures on the compact Riemann surface, are solved by choosing the  $A_i$  and  $B_j$  to all be of the same length. Varying the length of the opposing zero height sides of the rectangular domain yields a one-parameter family of surfaces.  $\square$

On the other hand, we immediately have:

**Corollary 4.2.**  *$M_k$  is a  $k$ -fold covering of  $M_1$ .*

*Proof.* Schwarz reflection (Theorem 3.1) about line segments on the bounding conjugate contour for  $M_1$  produces the bounding conjugate contour for  $M_k$  for any  $k$ . The uniqueness of the minimal graphs in Theorem 3.3 completes the proof.  $\square$

We included these examples  $M_k$  because the technique used to solve the  $k$ -dimensional period problem arising from the additional ends is used throughout the paper. In particular:

**Lemma 4.3.** *Each collection of surfaces,  $M_k^+, M_k^-, M_{2k+1}^{++}, M_{2k+1}^{--}, M_k^{+-}$ , results from adding ends and handles to  $M_1$ , and the period problems arising from the additional ends are all solved as above, that is, by requiring*

$$\varepsilon = \text{length } A_i = \text{length } B_j$$

*to be constant for all  $i, j$ .*

A proof of this lemma is contained in the appendix of this paper.

The observation that this restriction on the conjugate contour solves all the periods arising from additional ends demonstrates that these periods are independent of the periods arising from additional handles. This restriction enables us to eliminate all but one or two periods in these surfaces, so we may focus only on the periods arising from the new handles.

### 5. THE EXAMPLES $M_k^+$

The sketch in Figure 6, top is of a contour suggestive of a ‘+’ type handle in an even ended surface which we will use to motivate the discussion. Taking its conjugate contour produces the contour in Figure 6, middle, which is bounded by line segments as labelled in the figure. This contour bounds a Jenkins–Serrin graph over the front face of the box and hence supports a solution to the Plateau problem. Let  $\beta_j = \text{length } B_j = \text{length } B_j^*$  for  $j = 2, 3, 4, 5$ . The symmetries of  $M_k^+$  imply there are  $k$  periods,  $k - 1$  of these resulting from the ends, and one arising from the new handle. Lemma 4.3 implies that if we restrict the conjugate contours so that the lengths of the segments over which the boundary contour is unbounded are equal, then  $k - 1$  of these periods are zero. Let  $\varepsilon = \beta_3/k$  be this common length.

The remaining period is shown to change sign as  $\beta_4$  varies, so the intermediate value theorem implies:

**Theorem 5.1.** *For each  $k > 0$ , there exists a one-parameter family  $M_k^+$  of embedded, doubly periodic minimal surfaces of genus two with  $4k$  Scherk type ends.*

We give the argument only for the case  $k = 2$ , as the argument is essentially identical for all  $k$ . Choosing the curves  $B_2^*$  and  $B_3^*$  to lie at the zero level, the height of  $B_5^*$  is  $+\beta_4$ , with the end  $E_1^*$  at height  $+\infty$  and  $E_2^*$  at  $-\infty$  as indicated in Figure 6, bottom.

*Proof.* All that remains to be shown is that as  $\beta_4$  is varied, the period  $\pi(\beta_4) = \text{Re} \int_{S_1}^{V_4} \varphi_2$  changes signs. Note that this period measures the distance between the planes containing the curves  $B_4$  and  $C$ .

Let  $\beta_2 > \varepsilon$  and consider the two cases of  $\beta_4$  large and  $\beta_4$  small:

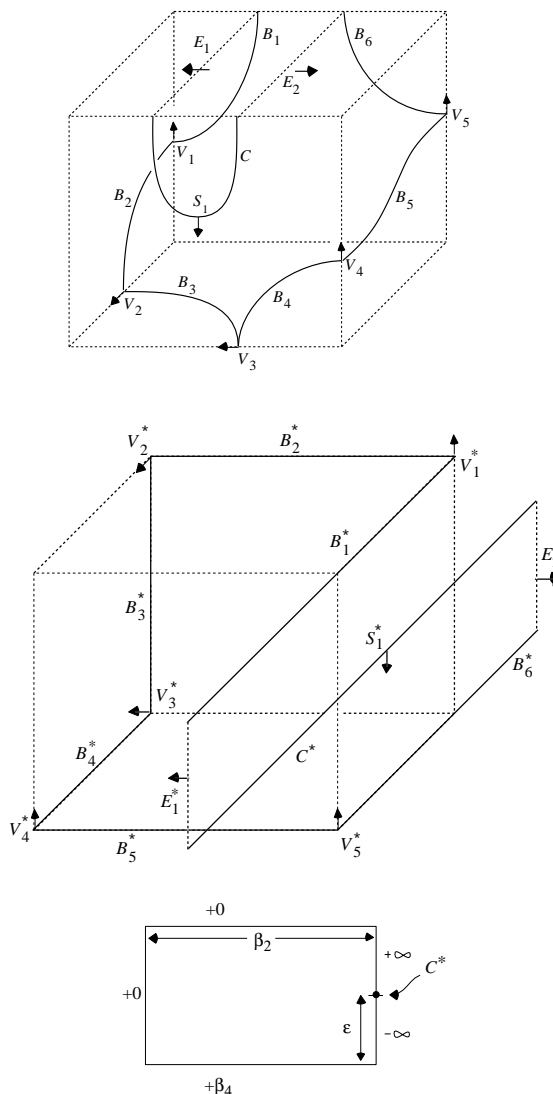


**FIGURE 6.** Sketches of the boundaries of one eighth of  $M_2^+$  and its conjugate (top and middle), and the graph dimensions and heights over the front face of the bounding box for the conjugate contour.

(a) Let  $\beta_4 \rightarrow 0$ . The limiting surface is  $M_2$  and the embeddedness of  $M_2$  implies the point  $V_4$  lies behind the symmetry plane of  $C$ ; so  $\pi(\beta_4) < 0$  for  $\beta_4$  near zero.

(b) For large  $\beta_4$ , we claim that the distance between the planes containing  $B_4$  and  $B_6$  is  $\beta_2 - \delta > \varepsilon$ , since the Gauss map approaches a constant along  $B_5$ . To see this, use the barrier surface given as a Jenkins–Serrin graph over the back face of the box in Figure 6, middle, with height  $+\infty$  over the edge  $B_5^*$  and the same heights as the contour for  $M_2^+$  over all other edges. Arguments in [Jenkins and Serrin 1966]

imply the conjugate graphs converge to the barrier surface as  $\beta_4 \rightarrow \infty$ . So in the limit, the behavior of the ends is the same and therefore  $B_5$  approaches a straight line of length  $\beta_2$  which is greater than  $\varepsilon$ . Hence  $B_4$  lies in front of  $C$  and  $\pi(\beta_4) > 0$  for  $\beta_4$  large.

Hence the period problem is solvable. Since  $\beta_2$  is only bounded below this shows the period problem can be solved for each  $\beta_2 > \varepsilon$  and therefore there exists a one-parameter family of these surfaces. Theorem 3.2 implies each eighth of any one of these surfaces is embedded and, by Theorem 3.1, extends to an embedded minimal surface.  $\square$

**Weierstrass Data for  $M_k^+$**

Since  $M_k^+$  is invariant under an order-two normal symmetry about the  $x_3$ -axis, with six fixed points, the quotient is a sphere minus  $2k$  points. The meromorphic function  $g^2$ , where  $g$  is the Gauss map, descends to the quotient. Taking  $z$  as the coordi-

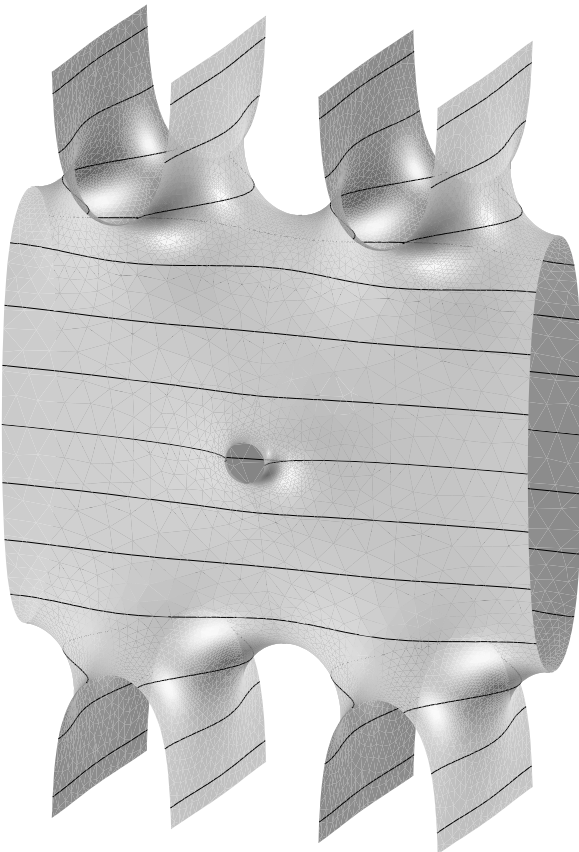


FIGURE 7. Fundamental piece of  $M_2^+$ .

nate on this sphere, we normalize so that  $z(V_3) = 0$ ,  $z(V_2) = \infty$  and  $e_k = z(E_k) = 1$ . Define  $v_i = z(V_i)$  for  $i = 1, 4, 5$  and  $s_j = z(S_j)$  for  $j = 1, 2, \dots, k-1$ , where  $\{S_j\}$  are the vertical points lying on the planar geodesics between the ends; further define  $e_m = z(E_m)$  for  $m = 1, \dots, k-1$ . Conformality of  $z$  orders these values thus:

$$0 < v_4 < v_5 < 1 < s_{k-1} < e_{k-1} < s_{k-2} < \dots < s_1 < e_1 < v_1.$$

Set

$$N_k(z, s_1, \dots, s_{k-1}) := \prod_{j=1}^{k-1} (z + (-1)^{k+j} s_j),$$

$$D_k(z, s_1, \dots, s_{k-1}) := \prod_{j=1}^{k-1} (z - (-1)^{k+j} s_j),$$

$$\mathcal{E}_k(z, e_1, \dots, e_k) := \prod_{m=1}^k (z^2 - e_m^2),$$

$$f_k(z, s_1, \dots, s_{k-1}) := \frac{N_k(z, s_1, \dots, s_{k-1})}{D_k(z, s_1, \dots, s_{k-1})}.$$

Comparison of the meromorphic functions  $g^2$  and  $z$  leads to these Weierstrass data for  $M_k^+$ :

$$g^2 = \frac{z+v_4}{z-v_4} \frac{z+v_5}{z-v_5} \frac{z+(-1)^k v_1}{z-(-1)^k v_1} f_k^2(z, s_1, \dots, s_{k-1}) \tag{5-1}$$

and

$$\eta = dz \frac{D_k(z, s_1, \dots, s_{k-1}) N_k(z, s_1, \dots, s_{k-1})}{\mathcal{E}_k(z, e_1, \dots, e_k)}. \tag{5-2}$$

The conditions for embedded ends are

$$g^2(1) = g^2(e_m) = 1 \tag{5-3}$$

for all  $m \leq k$ . For  $k = 2$ , we have the constraints

$$A(1 + v_4)(1 + v_5) = \tilde{A}(1 - v_4)(1 - v_5)$$

$$B(e_2 + v_4)(e_2 + v_5) = \tilde{B}(e_2 - v_4)(e_2 - v_5),$$

where  $A = (1 - s_1)^2(1 + v_1)$ ,  $\tilde{A} = (1 + s_1)^2(1 - v_1)$ ,  $B = (e_1 - s_1)^2(e_1 + v_1)$ , and  $\tilde{B} = (e_1 + s_1)^2(e_1 - v_1)$ . From this, we can derive the conditions

$$v_4 v_5 = \frac{(A - \tilde{A})(B + \tilde{B})e_1 - (A + \tilde{A})(B - \tilde{B})e_1^2}{(A + \tilde{A})(B - \tilde{B}) - (A - \tilde{A})(B + \tilde{B})e_1} \tag{5-4}$$

and

$$v_4 + v_5 = \frac{(A - \tilde{A})(B + \tilde{B})(e_1^2 - 1)}{(A + \tilde{A})(B - \tilde{B}) - (A - \tilde{A})(B + \tilde{B})e_1}, \tag{5-5}$$

and so solve for  $v_4$  and  $v_5$  as the zeros of a degree-two polynomial.

With the Weierstrass data (5-1), (5-2) and the constraints (5-4) and (5-5) we get the image in Figure 7 after choosing  $k = 2$  and determining the correct values for  $v_1$  and  $e_1$ .

**6. THE EXAMPLES  $M_k^-$**

The periods associated to  $M_k^-$  arise as residues at the punctures for the ends or from integrating along a curve representing a nontrivial homotopy class. As in the case of  $M_k$ , the residues at the ends are made equal by equally distributing the straight lines lying between the ends of the conjugate of one-eighth of the fundamental piece. The portion of the period problem resulting from nontrivial homotopy classes is one-dimensional due to the symmetries of  $M_k^-$ , and use of the same barriers as in [Wei 1992] shows that this period is also solvable. Hence:

**Theorem 6.1.** *There exists a one-parameter family of genus two, embedded minimal surfaces  $M_k^-$  with  $4k$  Scherk-type ends, for all  $k \geq 1$ .*

**7. THE EXAMPLES  $M_{2k+1}^{--}$**

In this section, we construct the embedded minimal surfaces  $M_{2k+1}^{--}$ . Specifically, we construct genus three surfaces having all the symmetries of Karcher’s genus one surface  $M_1$ , with two ‘-’ handles and  $4(2k + 1)$  Scherk ends.

F. Wei modified  $M_1$  by introducing a single handle over one of its saddle points. In the sketches of Figure 5, one can see that this results in a new vertical point over  $V_4$ . In order to retain the vertical straight lines of  $M_1$  on higher genus surfaces, one is obliged to add a handle over the other saddle point, since, by Theorem 3.1,  $180^\circ$  rotation about these straight lines are isometries of the surface. Such a surface might have a boundary like that sketched in Figure 8, left. If this surface did exist, its conjugate contour would be as in Figure 8, lower left. This conjugate contour meets all the conditions of Theorem 3.3, hence it supports a solution to the

Plateau Problem, and the original surface conjugate to this solution is a minimal surface bounded by planar curves with the desired symmetries.

Although the conjugate surface is a minimal surface bounded by planar curves, it is not guaranteed that reflection in these planes produces an embedded doubly periodic surface. In particular, using the notation of Figure 8, one does not know if the curves  $B_1$  and  $B_3$  lie in the same plane. This brings us to the period problem; one must insure that the planes containing  $B_1$  and  $B_3$  coincide. Since we have assumed the surface contains a vertical straight line, knowing  $B_1$  and  $B_3$  lie in the same plane implies the planes containing  $B_5$  and  $B_7$  also coincide. Should this period problem be solvable, the surface in our notation would be denoted by  $M_1^{--}$ .

In Theorem 7.1.2 we prove, by analyzing the Plateau solutions for the contour of Figure 8, lower left, that this period problem can never be solved. In contrast, by having more ends on the surface, as in Figure 8, right, we prove in Theorem 7.1.1 that the obstruction to solving this period problem is removed. These new surfaces are the surfaces  $M_{2k+1}^{--}$  in our notation.

- Theorem 7.1.** 1. *For each  $k \geq 1$ , there exists a one-parameter family of embedded, doubly periodic minimal surfaces  $M_{2k+1}^{--}$  of genus three.*  
 2.  $M_1^{--}$  does not exist.

*Proof.* Let  $\beta_j = \text{length } B_j = \text{length } B_j^*$  for  $j = 2, 3, 4, 5, 6$ . By Lemma 4.3, all periods arising from the addition of ends are zero provided the lengths of the segments over which the conjugate contours are unbounded are equal. We assume this condition, and let  $\varepsilon$  be this common length, which remains fixed throughout the proof. Hence we need only address the periods arising from nontrivial homotopy classes, that is, from the addition of new handles. From the conjugate contour one sees that  $\beta_4 = (2k + 1)\varepsilon$  for each  $M_{2k+1}^{--}$ .

*Proof of 2.* We proceed by contradiction. Suppose  $M_1^{--}$  does exist. Let  $S$  be one eighth of  $M_1^{--}$ . Figure 8, left shows a sketch of  $S$ . We are assuming that there is a vertical straight line on  $S$  passing through the end  $E$ , orthogonal to the plane containing  $B_4$ . Rotation about this line interchanges  $V_1$  and  $V_6$ , and interchanges  $V_2$  and  $V_5$ .

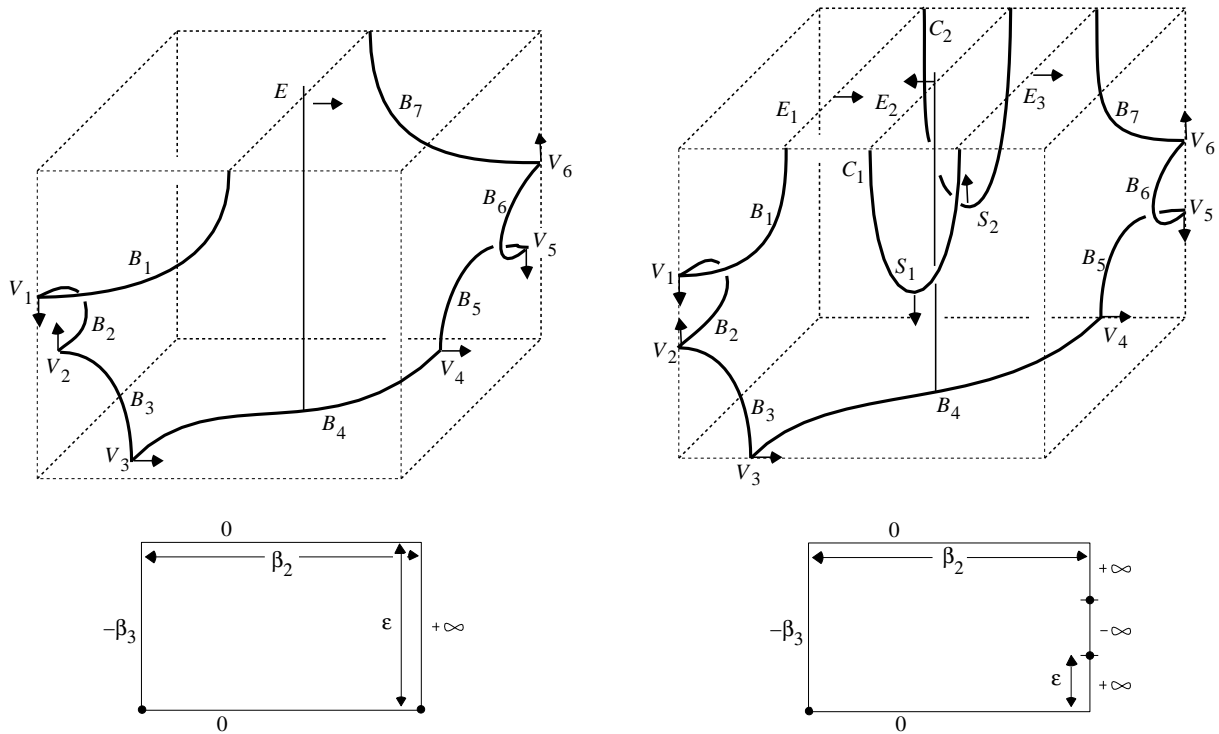


**FIGURE 8.** Sketches of the boundary of one eighth of  $M_1^{-}$  (upper left) and  $M_3^{-}$  (upper right) with the parameters for the conjugate boundary contour viewed as a graph over the rectangular region drawn below each sketch.

**Remark 7.2.** The boundary contour of  $S^*$  is a graph over a rectangle as drawn in Figure 8, lower left, and as a result of the symmetries,  $B_2^*$  and  $B_6^*$  lie at the same height. Choosing this to be the zero height implies the line  $B_4^*$  has height  $-\infty < -\beta_3 < 0$ , and the end  $E$  has height  $+\infty$ . From Theorem 3.3, we get a minimal graph with this boundary. As a graph, it is embedded and Theorem 3.2 assures that  $S$  is embedded. Hence there exists a Plateau solution  $S^*$  with the desired boundary and symmetries.

**Claim 1.** *The distance between the planes containing  $B_3$  and  $B_5$  is always shorter than the distance between the planes containing  $B_1$  and  $B_7$ . Hence the period is always of the same sign.*

The planar geodesic  $B_4$  has length  $\epsilon$  and is not a straight line. Therefore the distance between the symmetry planes containing  $B_3$  and  $B_5$  is strictly less than  $\beta_4 = \epsilon$ , and the curve  $B_3$  always lies to one side of the plane containing  $B_1$ . This establishes the claim and completes the proof of (2).

In summary, the period problem on  $M_1^{-}$  is unsolvable because the distance  $\epsilon$  between the planar curves bounding the end is equal to  $\beta_4$  and the planar curve  $B_4$  is not straight. If one could modify the

conjugate contour so that  $\beta_4 > \epsilon$ , then the period problem may be solvable. One way of achieving this is to add more ends to the conjugate contour as in the sketch in Figure 8, lower right. Because we wish to maintain the vertical straight lines, the contour bounded by straight lines must have a horizontal planar symmetry. Therefore we must add an even number of extra ends. Figure 8, right is a sketch of such a surface with three ends. The conjugate contour for this surface is again a Jenkins–Serrin graph over a rectangle as drawn in Figure 8, lower right.

**Proof of 1.** Assume  $\beta_2 > \beta_4 = (2k + 1)\epsilon$ . Since we have assumed the existence of a vertical straight line on the surface passing thru  $E_{k+1}$  and orthogonal to  $B_4$ , we have only one period arising from a nontrivial homotopy class. For this period, we must show that  $B_1$  lies in the plane containing  $B_3$ . We use the intermediate value theorem to show the existence of a value for  $\beta_3$  such that this period is zero. Specifically, we have two cases:

(a) As  $\beta_3 \rightarrow 0$ ,  $M_{2k+1}^{-}$  degenerates to  $M_{2k+1}$ . By the embeddedness of  $M_{2k+1}$ , we have the point  $V_2$  moves behind the plane containing  $B_1$ , and the period is negative.

(b) As  $\beta_3 \rightarrow \infty$ , the curve  $B_4^*$  moves away toward height  $-\infty$ . Let  $\mathcal{B}$  be the Jenkins–Serrin graph over the rectangle as described in Figure 8, lower right, with boundary heights  $0, -\infty, 0, +\infty, -\infty, +\infty$  with zero heights corresponding to the edges containing the curves  $B_2^*$  and  $B_6^*$ . This graph  $\mathcal{B}$  exists, since  $\beta_2 > \beta_4$ , by Theorem 3.3. By the arguments in [Jenkins and Serrin 1966], the conjugate graphs converge to  $\mathcal{B}$  as  $\beta_3 \rightarrow \infty$ . Therefore along  $B_4^*$  the Gauss map approaches a constant value, and the displacement along  $B_4$  in the desired direction approaches  $(2k+1)\varepsilon = \beta_4$ . Hence  $V_2$  lies in front of the plane containing  $B_1$  for large  $\beta_3$ , and the period is positive.

By the intermediate value theorem, there exists a value of  $\beta_3$  at which the period is zero. Therefore the period problem is solvable on  $M_{2k+1}^{--}$ .

Theorems 3.3 and 3.2 imply that the one eighth portion  $S$  of  $M_{2k+1}^{--}$  is embedded. Applying the classical maximum principle and the maximum principle at infinity [Meeks and Rosenberg 1990], one easily determines that the full fundamental piece of  $M_{2k+1}^{--}$  lies inside the box given by its boundary curves. Reflections through the faces of this box produces an embedded surface. Therefore  $M_{2k+1}^{--}$  is embedded.

$\beta_2$  has not been used in this argument ( $\beta_2$  is any fixed number greater than  $\beta_4$ ), and therefore we have a one-parameter family of  $M_{2k+1}^{--}$  for each  $k \geq 1$ .  $\square$

### Weierstrass Data for $M_3^{--}$

Since  $M_3^{--}$  is invariant under an order-two normal symmetry about the  $x_3$ -axis, with eight fixed points, the quotient surface is a sphere. The meromorphic function  $g^2$ , where  $g$  is the stereographic projection of the Gauss map, descends to the quotient. Taking  $z$  to be the coordinate on the sphere, we normalize so that  $z(V_3) = \infty$ ,  $z(V_4) = 0$ , and  $z(E_2) = 1$ . With this normalization, rotation about the vertical straight line on  $M_3^{--}$  corresponds to inversion through the unit circle. Define  $e_1 = z(E_1)$ ,  $v_j = z(V_j)$  for  $j = 1, 2$ , and  $s_1 = z(S_1)$ . Then  $z(E_3) = 1/e_1$ ,  $z(V_5) = 1/v_2$ ,  $z(V_6) = 1/v_1$ , and  $z(S_2) = 1/s_1$ . Comparison of the meromorphic functions  $g^2$  and  $z$  leads to these Weierstrass data for  $M_3^{--}$ :

$$g^2 = \frac{z-v_1}{z+v_1} \frac{z+1/v_1}{z-1/v_1} \frac{z+v_2}{z-v_2} \frac{z-1/v_2}{z+1/v_2} \left( \frac{z-s_1}{z+s_1} \right)^2 \left( \frac{z+1/s_1}{z-1/s_1} \right)^2$$

and

$$\eta = \frac{dz}{z^2-1} \frac{z^2-s_1^2}{z^2-e_1^2} \frac{z^2-1/e_1^2}{z^2-1/e_1^2}.$$

These Weierstrass data insure that each Scherk-type end is itself an embedded end, but one must also guarantee that the limit normals on the ends are antipodal so the ends do not cross each other as they diverge. Because of our choice of orientation, this is equivalent to the conditions

$$g^2(1) = g^2(e_1) = g^2(1/e_1) = 1.$$

Due to the rotational symmetry, the second and third conditions result in the same constraints, while the first is automatically satisfied. The second condition places the following constraint on  $e_1$ :

$$\begin{aligned} &(\delta+\gamma+2\nu)e_1^6 \\ &+ ((\delta+\gamma)(\nu^2-1)+2(\delta\gamma-2)\nu-(\delta+\gamma)-2\nu)e_1^4 \\ &+ (2\nu-(\delta+\gamma)(\nu^2-2)-2\nu(\delta\gamma-2)+(\delta+\gamma))e_1^2 \\ &- 2\nu - (\delta+\gamma) = 0, \quad (7-1) \end{aligned}$$

where  $\delta = v_2 - 1/v_2$ ,  $\gamma = 1/v_1 - v_1$ , and  $\nu = 1/s_1 - s_1$ .

By Theorem 7.1, there exists a solution to (7-1) in the necessary range. Using the computer to find this solution and to calculate the values of the two periods of the Weierstrass data, we determine the appropriate values for  $e_1$ ,  $v_1$ , and  $v_2$ , given a value for  $s_1$ . We thereby generate the image of  $M_3^{--}$  in Figure 2.

### 8. THE EXAMPLES $M_{2k+1}^{++}$

As in the previous section, one might investigate whether it is possible to construct genus three examples by adding two ‘+’ type handles to  $M_1$  while preserving the symmetries. The same methods as those used in the ‘-’ case can be used to show the existence of a minimal disc with the desired boundary and symmetries, but one must again consider the period problem. The similarities between the conjugate contours for the two ‘-’ handles and two ‘+’ handles allow one to observe a similar natural obstruction to solving the period problem for the one-ended surfaces. By adding more ends to these surfaces, as in the previous section, this obstruction is overcome. Denoting these new surfaces by  $M_{2k+1}^{++}$  and using arguments similar to those used in the proof of Theorem 7.1, one has:

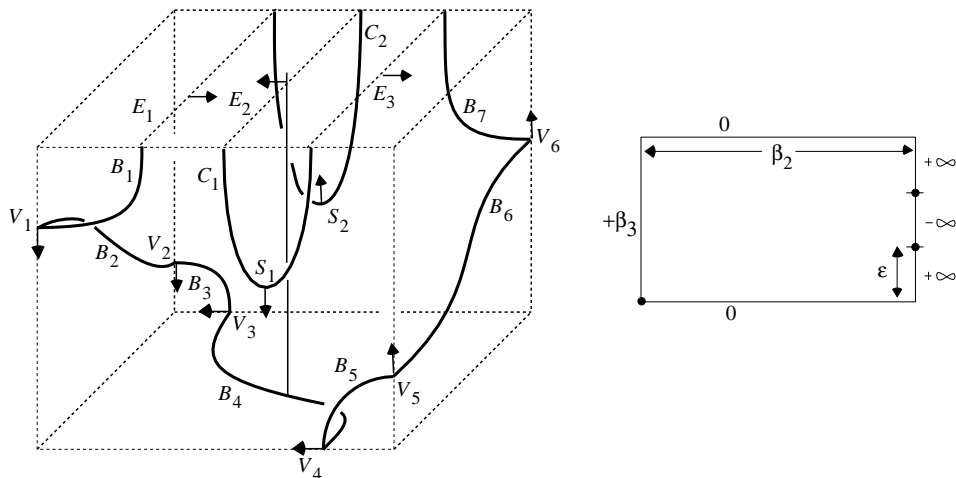


FIGURE 9. Sketches of the boundary of one eighth of  $M_3^{++}$  and its conjugate boundary graph heights over the front face of the bounding box.

**Theorem 8.1.** 1. *There exists a one-parameter family of embedded, doubly periodic minimal surfaces  $M_{2k+1}^{++}$  of genus three, for each  $k \geq 1$ .*  
 2.  $M_1^{++}$  does not exist.

**Remark 8.2.** The symmetry groups for  $M_1$ ,  $M_{2k+1}^{--}$ , and  $M_{2k+1}^{++}$  are identical. Hence one has two collections of genus three minimal surfaces with the same symmetries as Karcher’s original genus one surface

**Weierstrass Data for  $M_3^{++}$**

Using the same notation as that used for the surface  $M_3^{--}$ , we can determine the Weierstrass data for  $M_3^{++}$ ; the results are

$$g^2 = \frac{z-v_1}{z+v_1} \frac{z+1/v_1}{z-1/v_1} \frac{z-v_2}{z+v_2} \frac{z+1/v_2}{z-1/v_2} \left( \frac{z-s_1}{z+s_1} \right)^2 \left( \frac{z+1/s_1}{z-1/s_1} \right)^2$$

$$\eta = \frac{dz}{z^2-1} \frac{z^2-s_1^2}{z^2-e_1^2} \frac{z^2-1/e_1^2}{z^2-1/e_1^2}$$

With the same constraints for parallel ends as in (7-1) and by changing  $\gamma$  to  $v_1 - 1/v_1$  we compute the parameters used in generating the image in Figure 2.

**9. THE EXAMPLES  $M_k^{+-}$**

In this section, we consider the genus three surfaces  $M_k^{+-}$  which arise by adding both a ‘+’ handle and a ‘-’ handle to  $M_k$ . As in the case of  $M_k^-$  and  $M_k^+$ , the handles make it impossible to preserve the straight line symmetries of  $M_1$ , but the three mutually perpendicular planar reflectional symmetries are preserved. These symmetries reduce the number

of periods that need to be addressed in order for the period problem to be solved. In particular,  $M_k^{+-}$  has  $k + 1$  periods:  $k - 1$  of these periods arise from the residues of the Weierstrass data at the ends; leaving only two periods resulting from nontrivial homotopy classes. By Lemma 4.3, the periods resulting from the additional ends are simultaneously zero provided the segments over which the conjugate contours are unbounded are equal in length. As we have done in the previous sections, we fix  $\epsilon$  to be this common length. Now we need only consider the two periods that result from nontrivial homotopy classes.

Figure 10 contains sketches of the boundary of one eighth of  $M_2^{+-}$  (left) and  $M_3^{+-}$  (right), together with the conjugate contour heights written as a graph, where  $\beta_j = \text{length } B_j$  for  $j = 2, 3, 4, 5, 6$ . We assume  $\beta_2 > \epsilon$  on all contours.

We now consider the case  $k = 1$ . By consideration of the two periods for  $M_1^{+-}$  for varying values of  $\beta_3$  and  $\beta_5$ , we are able to use a two-dimensional degree argument to prove:

**Theorem 9.1.** *There exists a one-parameter family of genus three, embedded minimal surfaces  $M_1^{+-}$  with 4 Scherk-type ends.*

In particular, consider the periods along the curves in the  $(\beta_3, \beta_5)$  plane given by

$$\begin{aligned} \tau_1 &= (0, \beta_5) \quad \text{for } \beta_5 \in [0, T], \\ \tau_2 &= (\beta_3, T) \quad \text{for } \beta_3 \in [0, S], \\ \tau_3 &= (S, \beta_5) \quad \text{for } \beta_5 \in [0, T], \\ \tau_4 &= (\beta_3, 0) \quad \text{for } \beta_3 \in [0, S], \end{aligned}$$

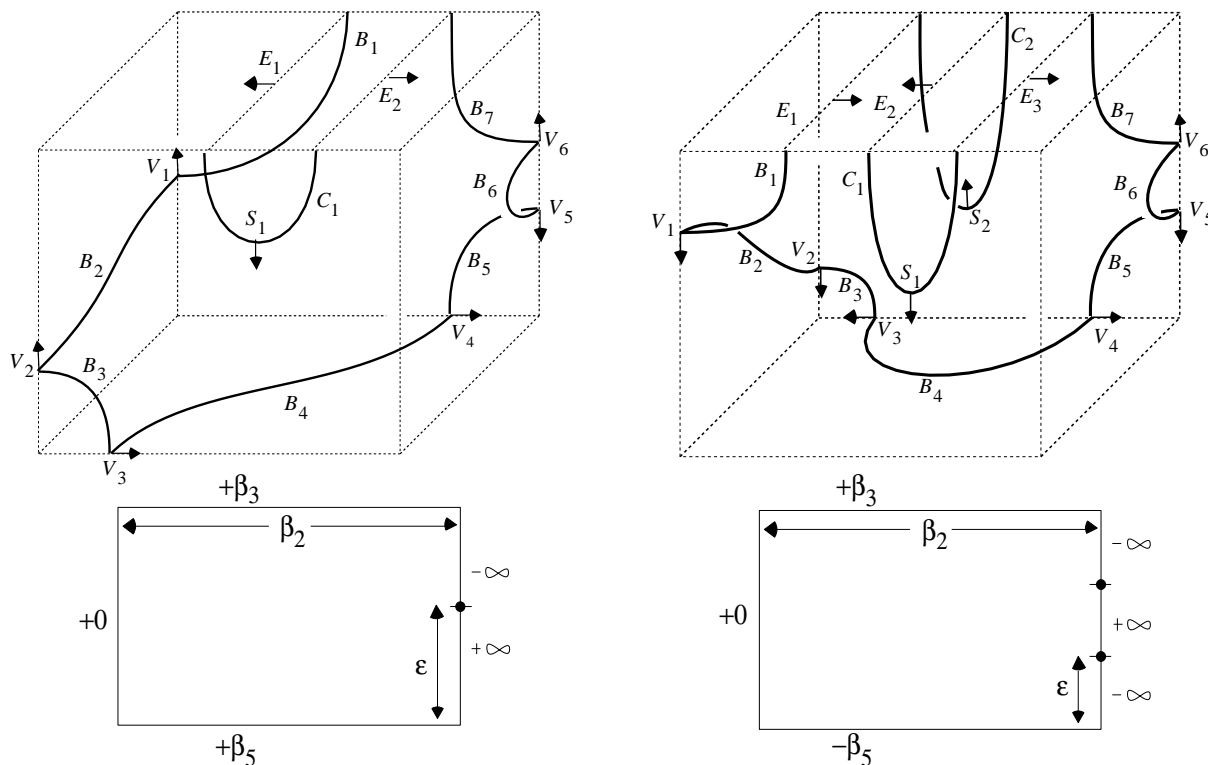


FIGURE 10. Sketches of one eighth of  $M_2^{+-}$  (upper left) and  $M_3^{+-}$  (upper right) with the Jenkin–Serrin graph boundary heights for the conjugates of each eighth drawn below.

for positive  $S$  and  $T$ , and are able to show that, with the correct choices for  $\beta_2$ ,  $S$ , and  $T$ , these curves surround a solution for the period problem.

The conjugate contours for  $M_1^{+-}$  associated to points along the curves  $\tau_1$  and  $\tau_4$  degenerate to conjugate contours for either known surfaces or surfaces which are known to have unsolvable period problems. When the degenerate contour is known to have a solvable period problem, we assume nothing about the values of these periods, and in general the remaining unfixed parameter which we will not specify has been shown to control this period. We seek to use only the general shape of the degenerate contours and not the solvability of the period problems on the lower genus minimal surfaces. On each of the degenerate surfaces, the labels we use are inherited from the contour for  $M_1^{+-}$ , which may differ from those used previously in the text.

*Proof of Theorem 9.1.* Consider one-eighth of the fundamental piece, analogous to the depictions of  $M_2^{+-}$  and  $M_3^{+-}$  in Figure 10. This one-eighth piece is bounded by seven planar geodesics  $B_1, \dots, B_7$ .  $B_1$  and  $B_7$  are each of infinite length with a single end-

point, and  $B_2, \dots, B_6$  are each finite length curve segments. Let  $\beta_j = \text{length } B_j$  for  $j = 2, 3, 4, 5, 6$ . The singular points of the boundary are  $V_j = B_j \cap B_{j+1}$  for  $j = 1, \dots, 6$ . (Unlike the cases when  $k \geq 2$ , there are no curves  $C_j$ , as in Figure 10.) We place the surface so that  $g$  equals 1 at the single end  $E_1$  and equals 0 at  $V_1$ , and we define the functions

$$\begin{aligned} \pi_1(\beta_2, \beta_3, \beta_5) &= \text{Re} \int_{V_3}^{V_4} \varphi_2 = \text{Re} \int_{V_2}^{V_4} \varphi_2, \\ \pi_2(\beta_2, \beta_3, \beta_5) &= \text{Re} \int_{V_4}^{V_6} \varphi_2 = \text{Re} \int_{V_5}^{V_6} \varphi_2, \end{aligned}$$

where  $\varphi_2$  is the second component of the Weierstrass map given in equation (3–2). We will show that:

- (i)  $\pi_1(\tau_j)$  and  $\pi_2(\tau_j)$  change monotonically on each  $\tau_j$ , for  $j = 1, 2, 3, 4$ . In particular, for each fixed  $\beta_2$  and  $\beta_5$ ,  $\pi_1(\beta_2, \beta_3, \beta_5)$  is a strictly decreasing function of  $\beta_3$ ; for each fixed  $\beta_2$  and  $\beta_3$ , the value  $\pi_1(\beta_2, \beta_3, \beta_5)$  is a strictly increasing function of  $\beta_5$ ; for each fixed  $\beta_2$  and  $\beta_5$ ,  $\pi_2(\beta_2, \beta_3, \beta_5)$  is a strictly decreasing function of  $\beta_3$ ; and for each fixed  $\beta_2$  and  $\beta_3$ ,  $\pi_2(\beta_2, \beta_3, \beta_5)$  is a strictly decreasing function of  $\beta_5$ .

- (ii) For all  $\beta_2 > \varepsilon$ ,  $\pi_1(\beta_2, 0, 0) > 0$  and  $\pi_2(\beta_2, 0, 0) > 0$ .
- (iii) For any fixed  $\beta_2 > \varepsilon$ , if  $T$  is chosen sufficiently large, then  $\pi_1(\beta_2, 0, T) > 0$  and  $\pi_2(\beta_2, 0, T) < 0$ .
- (iv) There exist choices for  $\beta_2 > \varepsilon$  and  $S$  large so that  $\pi_1(\beta_2, S, 0) < 0$  and  $\pi_2(\beta_2, S, 0) = 0$ .

We consider the period map

$$\Pi(\beta_2, \beta_3, \beta_5) = (\pi_1(\beta_2, \beta_3, \beta_5), \pi_2(\beta_2, \beta_3, \beta_5)).$$

We choose  $\beta_2$ ,  $S$ , and  $T$  so that  $\pi_1(\beta_2, 0, T) > 0$ ,  $\pi_2(\beta_2, 0, T) < 0$ ,  $\pi_1(\beta_2, S, 0) < 0$ , and  $\pi_2(\beta_2, S, 0) = 0$ . Since  $\beta_2$  is then a fixed value, we may consider  $\pi_1 = \pi_1(\beta_3, \beta_5)$  and  $\pi_2 = \pi_2(\beta_3, \beta_5)$  as functions of only the two variables  $\beta_3$  and  $\beta_5$ . Hence  $\Pi$  is a map from  $\mathbb{R}^2$  to  $\mathbb{R}^2$ . By the monotonic behavior of  $\pi_1$  and  $\pi_2$  on each  $\tau_j$ , it follows that the image of  $\tau_1 \cup \tau_2 \cup \tau_3 \cup \tau_4$  under  $\Pi$  is a homotopically nontrivial loop in  $\mathbb{R}^2 \setminus \{(0, 0)\}$ . Thus a zero for the period map  $\Pi$  lies in the region bounded by the curves  $\tau_j$ . Hence the period problem associated to  $M_1^{+-}$  is solvable.

We prove items (i)–(iv) above by studying the conjugate surface of the original one-eighth portion bounded by planar geodesics  $B_1, \dots, B_7$ . The conjugate surface is a graph  $\mathcal{B}$  with respect to the  $x_2$  direction over the rectangle

$$\{(x_1, 0, x_3) \in \mathbb{R}^3 : 0 \leq x_1 \leq \beta_2, 0 \leq x_3 \leq \varepsilon\}$$

in the  $x_1x_3$ -plane, and its boundary, the conjugate contour, consists of seven lines  $B_1^*, \dots, B_7^*$  corresponding to the planar geodesics  $B_1, \dots, B_7$  in the boundary of the original surface. Since conjugation preserves lengths, we have  $\beta_j = \text{length } B_j = \text{length } B_j^*$ . Thus  $B_1^*$  and  $B_7^*$  are each infinite rays with a single endpoint, and  $B_2^*, \dots, B_6^*$  are each finite line segments. The singular points of the conjugate contour are  $V_j^* = B_j^* \cap B_{j+1}^*$  for  $j = 1, \dots, 6$ , corresponding to the points  $V_j$  on the original surface.  $B_1^*$  is the ray with endpoint  $(\beta_2, -\beta_3, \varepsilon)$  pointing in the direction of the positive  $x_2$ -axis.  $B_2^*$  is the segment with endpoints  $(\beta_2, -\beta_3, \varepsilon)$  and  $(0, -\beta_3, \varepsilon)$ .  $B_3^*$  is the line segment with endpoints  $(0, -\beta_3, \varepsilon)$  and  $(0, 0, \varepsilon)$ .  $B_4^*$  is the line segment with endpoints  $(0, 0, \varepsilon)$  and  $(0, 0, 0)$ .  $B_5^*$  is the line segment with endpoints  $(0, 0, 0)$  and  $(0, \beta_5, 0)$ .  $B_6^*$  is the line segment with endpoints  $(0, \beta_5, 0)$  and  $(\beta_2, \beta_5, 0)$ .  $B_7^*$  is the ray with endpoint  $(\beta_2, \beta_5, 0)$  pointing in the direction of the positive  $x_2$ -axis.

We denote this conjugate graph by  $\mathcal{B}(\beta_2, \beta_3, \beta_5)$ , since it depends on the values of  $\beta_2, \beta_3$  and  $\beta_5$ . (It also depends on  $\varepsilon$ , but  $\varepsilon$  will remain fixed, so we do not notate this dependence.)

Proof of (i). Choose nonnegative values  $\beta_3, \tilde{\beta}_3$ , and  $\beta_5$ , with  $\beta_3 < \tilde{\beta}_3$ , and choose any  $\beta_2 > \varepsilon$ . Then the interior of the graph  $\mathcal{B}(\beta_2, \beta_3, \beta_5)$  lies above the interior of  $\mathcal{B}(\beta_2, \tilde{\beta}_3, \beta_5)$  with respect to the  $x_2$  direction, by Remark 3.4. These two graphs have the line  $B_4^*$  in common, and it follows that as one travels from  $V_3^*$  to  $V_4^*$  along  $B_4^*$ , the normal vector along  $B_4^*$  of  $\mathcal{B}(\beta_2, \beta_3, \beta_5)$  is turning ahead of the normal vector along  $B_4^*$  of  $\mathcal{B}(\beta_2, \tilde{\beta}_3, \beta_5)$ . Furthermore, by the maximum principle these two normal vectors can never be equal in the interior of  $B_4^*$ . This means that on the original surfaces the normal vector along  $B_4$  for  $\beta_2, \beta_3, \beta_5$  is turning strictly ahead of the normal vector along  $B_4$  for  $\beta_2, \tilde{\beta}_3, \beta_5$ , with respect to arc length. Since  $\text{length } B_4 = \text{length } B_4^* = \beta_4 = \varepsilon$  is independent of  $\beta_3$ , it follows that  $\pi_1(\beta_2, \beta_3, \beta_5) > \pi_1(\beta_2, \tilde{\beta}_3, \beta_5)$ .

We have just shown that for each fixed  $\beta_2$  and  $\beta_5$ ,  $\pi_1$  is a strictly decreasing function of  $\beta_3$ . Similar arguments show the other parts of (i).

Proof of (ii). If  $\beta_3 = \beta_5 = 0$ , then  $V_2$  coincides with  $V_3$  and  $V_4$  coincides with  $V_5$ . The conjugate graph of this surface is unique, by Theorem 3.3, hence the surface is unique. Therefore it is  $M_1$ . The embeddedness of  $M_1$  implies that  $\pi_2(\beta_2, 0, 0) > 0$ .

The surface  $M_1$  contains a vertical line, and this line divides both  $M_1$  and  $B_4$  into two congruent pieces. Let  $\hat{B}_4$  be the half of  $B_4$  that connects the midpoint of  $B_4$  to  $V_3 = V_2$ . Let  $\hat{M}_1$  be the congruent piece of  $M_1$  bounded by  $B_1, B_2, \hat{B}_4$ , and the vertical line. Since  $\hat{M}_1$  has a single Scherk-type end whose normal is parallel to the  $x_1$  axis, the maximum principle implies that the  $x_2$  coordinate function on  $M_1$  cannot be maximized in the interior of  $M_1$ . Furthermore, as  $B_2$  is a planar geodesic in a plane parallel to the  $x_2x_3$ -plane, the boundary maximum principle implies that  $x_2$  cannot be maximized on  $B_2$ . Similarly,  $x_2$  cannot be maximized on the interior of  $\hat{B}_4$ . Therefore the value of the  $x_2$  coordinate at  $V_2 = V_3$  is strictly less than the value of the  $x_2$  coordinate at the midpoint of  $B_4$ . So  $\pi_1(\beta_2, 0, 0) > 0$ .

Proof of (iii). Fix  $\beta_2 > \varepsilon$ , and choose  $\beta_3 = 0$  and  $\beta_5 = T \gg 1$ . Then  $\lim_{T \rightarrow \infty} \mathcal{B}(\beta_2, 0, T)$  is a graph

bounded by  $B_1^*$ ,  $B_2^*$ ,  $B_4^*$ , and an infinite ray with endpoint at  $V_4^*$  pointing in the direction of the positive  $x_2$ -axis. This graph has a single Scherk-type end of width  $\sqrt{\beta_2^2 + \varepsilon^2}$ . (The fact that this limiting behavior occurs follows from the arguments in [Jenkins and Serrin 1966]. In this proof we will consider various limit surfaces, and in all cases the existence of the limit graph follows from [Jenkins and Serrin 1966].)

The original surface corresponding to

$$\lim_{T \rightarrow \infty} \mathcal{B}(\beta_2, 0, T)$$

via conjugation is bounded by the planar geodesics  $B_1$ ,  $B_2$ ,  $B_4$ , and an infinite version of  $B_5$ . It has a single nonvertical Scherk-type end of width  $\sqrt{\beta_2^2 + \varepsilon^2}$ . On  $\lim_{T \rightarrow \infty} \mathcal{B}(\beta_2, 0, T)$ , the maximum principle implies that its normal vector  $\vec{N}$  along  $B_4^*$  lies within a  $90^\circ$  geodesic arc of the unit sphere (so this is also true along  $B_4$ ), and thus the  $x_2$  coordinate at  $V_4$  is greater than the  $x_2$  coordinate at  $V_2 = V_3$  on the original surface, so  $\lim_{T \rightarrow \infty} \pi_1(\beta_2, 0, T) > 0$ . Hence  $\pi_1(\beta_2, 0, T) > 0$  for  $T$  sufficiently large.

Now we consider the limiting conjugate surface

$$\lim_{T \rightarrow \infty} (\mathcal{B}(\beta_2, 0, T) - (0, T, 0)),$$

which is a graph bounded by  $B_6^*$ ,  $B_7^*$ , an infinite version of  $B_5^*$  equal to the negative  $x_2$  axis, and a complete line through  $(\beta_2, 0, \varepsilon)$  parallel to the the  $x_2$ -axis. This conjugate surface has two ends of Scherk-type. One end has width  $\varepsilon$  and the other has width  $\sqrt{\beta_2^2 + \varepsilon^2}$ . The original surface that corresponds to it via conjugation is bounded by  $B_6$ ,  $B_7$ , an infinite version of  $B_5$ , and a complete infinite version of  $B_1$ . It has two ends, again of width  $\varepsilon$  and  $\sqrt{\beta_2^2 + \varepsilon^2} > \varepsilon$ . Because of the relative widths of the ends on this original surface, we see that the  $x_2$  coordinate at  $V_5$  is greater than the  $x_2$  coordinate at  $V_6$ , so  $\lim_{T \rightarrow \infty} \pi_2(\beta_2, 0, T) < 0$ . Hence  $\pi_2(\beta_2, 0, T) < 0$  for  $T$  sufficiently large. (See Figure 11.)

Proof of (iv). Choose  $\beta_2 > \varepsilon$ ,  $\beta_5 = 0$ , and  $\beta_3 = S \gg 1$ . We consider the limiting conjugate surface  $\lim_{S \rightarrow \infty} \mathcal{B}(\beta_2, S, 0)$ , which is a graph bounded by  $B_4^*$ ,  $B_6^*$ ,  $B_7^*$ , an infinite ray with endpoint at  $V_3^*$  pointing in the direction of the negative  $x_2$ -axis, and a complete line through  $(\beta_2, 0, \varepsilon)$  parallel to the the  $x_2$ -axis. This conjugate surface has two ends of Scherk-type. One end has width  $\varepsilon$  and the other

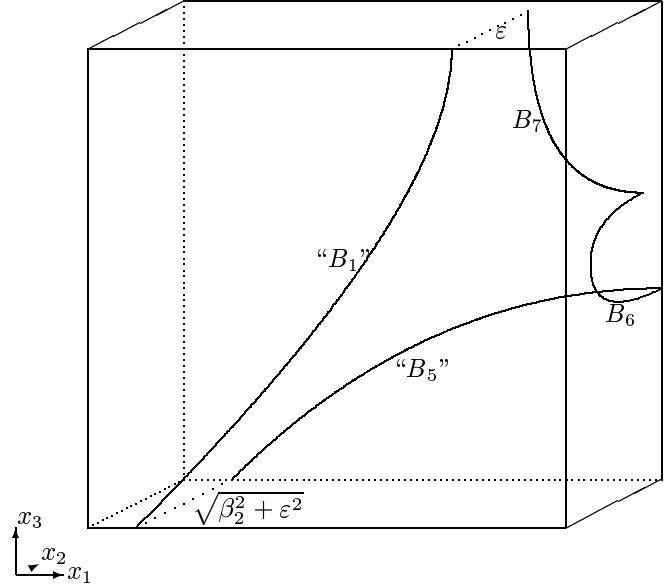


FIGURE 11. The original limit surface described at the end of the proof of (iii).

has width  $\beta_2$ . The original surface that corresponds to it via conjugation is bounded by  $B_4$ ,  $B_6$ ,  $B_7$ , an infinite ray version of  $B_3$ , and a complete infinite version of  $B_1$ . It has two ends, again one of width  $\varepsilon$  and the other of width  $\beta_2$ .

We now consider what happens to the original surface corresponding to  $\lim_{S \rightarrow \infty} \mathcal{B}(\beta_2, S, 0)$  as  $\beta_2 \searrow \varepsilon$  and as  $\beta_2 \nearrow \infty$ .

The conjugate surface  $\lim_{\beta_2 \rightarrow \varepsilon} (\lim_{S \rightarrow \infty} \mathcal{B}(\beta_2, S, 0))$  is a graph with respect to the  $x_2$  direction over the square  $\{(x_1, 0, x_3) \in \mathbb{R}^3 : 0 \leq x_1, x_3 \leq \varepsilon\}$ . It is bounded by the infinite ray  $B_7^*$  with endpoint  $(\varepsilon, 0, 0)$  pointing in the direction of the positive  $x_2$ -axis, the line segment  $B_6^*$  from  $(\varepsilon, 0, 0)$  to  $(0, 0, 0)$ , the line segment  $B_4^*$  from  $(0, 0, 0)$  to  $(0, 0, \varepsilon)$ , and the infinite ray with endpoint  $(0, 0, \varepsilon)$  pointing in the direction of the negative  $x_2$ -axis. The corresponding original surface is bounded by the planar geodesics  $B_4$ ,  $B_6$ ,  $B_7$ , and a complete infinite version of  $B_1$ . This original surface has two ends of Scherk-type, both of width  $\varepsilon$ .

Note that the graph  $\lim_{\beta_2 \rightarrow \varepsilon} (\lim_{S \rightarrow \infty} \mathcal{B}(\beta_2, S, 0))$  contains the line segment from  $(0, 0, 0)$  to  $(\varepsilon, 0, \varepsilon)$  and is symmetric with respect to rotation about this line, by uniqueness in Theorem 3.3 and by Theorem 3.1. The maximum principle then implies that the normal vector  $\vec{N}$  along each of  $B_4^*$  and  $B_6^*$  is contained in a  $90^\circ$  geodesic arc of the unit sphere, and

thus the  $x_2$  coordinate at  $V_3$  is greater than the  $x_2$  coordinate at  $V_4 = V_5$  in the corresponding original surface, and the  $x_2$  coordinate at  $V_3$  equals the  $x_2$  coordinate at  $V_6$ . Therefore

$$\lim_{\beta_2 \rightarrow \varepsilon} \left( \lim_{S \rightarrow \infty} \pi_2(\beta_2, S, 0) \right) = - \lim_{\beta_2 \rightarrow \varepsilon} \left( \lim_{S \rightarrow \infty} \pi_1(\beta_2, S, 0) \right) > 0.$$

Hence for  $\beta_2$  sufficiently close to  $\varepsilon$  and  $S$  sufficiently large, we have  $\pi_2(\beta_2, S, 0) > 0$ .

The limiting conjugate surface

$$\lim_{\beta_2 \rightarrow \infty} \left( \lim_{S \rightarrow \infty} \mathcal{B}(\beta_2, S, 0) \right)$$

is a portion of a helicoid (this follows from [Jenkins and Serrin 1966]) bounded by the positive  $x_1$ -axis, the line segment  $B_4^*$  from  $(0, 0, 0)$  to  $(0, 0, \varepsilon)$ , and an infinite ray with endpoint  $(0, 0, \varepsilon)$  pointing in the direction of the negative  $x_2$ -axis. On the corresponding original surface, one eighth of a catenoid, we then have that  $B_4$  is a quarter circle of radius  $2\varepsilon/\pi$ . Thus  $\lim_{\beta_2 \rightarrow \infty} (\lim_{S \rightarrow \infty} \pi_1(\beta_2, S, 0)) = -2\varepsilon/\pi$ . Since the original surface corresponding to

$$\lim_{S \rightarrow \infty} \mathcal{B}(\beta_2, S, 0)$$

has two Scherk-type ends of width  $\varepsilon$  and  $\beta_2$ , it follows that

$$\begin{aligned} \lim_{\beta_2 \rightarrow \infty} \left( \lim_{S \rightarrow \infty} (\pi_1(\beta_2, S, 0) + \pi_2(\beta_2, S, 0)) \right) \\ = \lim_{\beta_2 \rightarrow \infty} (\varepsilon - \beta_2) = -\infty. \end{aligned}$$

Thus for  $\beta_2$  and  $S$  sufficiently large, we have

$$\pi_2(\beta_2, S, 0) < 0.$$

Therefore for some large  $S$  and some value of  $\beta_2 > \varepsilon$ , we have  $\pi_2(\beta_2, S, 0) = 0$ . If, for this  $S$  and  $\beta_2$ , we have  $\pi_1(\beta_2, S, 0) \geq 0$ , then the original surface corresponding to this  $\beta_2$ ,  $\beta_3 = S$ , and  $\beta_5 = 0$  would contain some point in  $B_4 \cup B_6$  where  $x_2$  has a local maximum and where the tangent plane is parallel to the  $x_1x_3$ -plane. This contradicts the maximum principle. So, for this  $S$  and  $\beta_2$ , we have  $\pi_1(\beta_2, S, 0) < 0$ . This shows (iv).

This completes the proof of the solvability of the period problem associated to  $M_1^{+-}$ . Note that

$$\Pi(\tau_1 \cup \tau_2 \cup \tau_3 \cup \tau_4)$$

changes continuously under continuous changes of  $\beta_2$ , so for all  $\beta_2$  sufficiently close to the  $\beta_2$  chosen above,  $\Pi(\tau_1 \cup \tau_2 \cup \tau_3 \cup \tau_4)$  is still a homotopically

nontrivial loop in  $\mathbb{R}^2 \setminus \{(0, 0)\}$ , and so the period problem remains solvable. Hence  $\beta_2$  in a small open interval serves as a deformation parameter for the surface, thereby yielding a one-parameter family of these surfaces. Since each eighth of the surface is embedded, and the maximum principle tells us this embedded surface lies in the bounding box determined by the planar curves  $B_j$ , each surface in the family is embedded. This completes the proof.  $\square$

The proof of Theorem 9.1 cannot be directly adapted to prove existence of  $M_k^{+-}$  for  $k \geq 2$ . However, numerical evidence suggests that the  $M_k^{+-}$  exist for  $k \geq 2$  as well, so we make this conjecture (see Figure 3).

**Conjecture 9.2.** *There exists a one-parameter family of genus three, embedded minimal surfaces  $M_k^{+-}$  with  $4k$  Scherk-type ends, for all  $k \geq 2$ .*

Numerical evidence also suggests that there exists a wide variety of minimal surfaces with Scherk-type ends and more handles of both  $+$  and  $-$  type. (See Figure 12 for two genus 10 examples)

#### APPENDIX: A PROOF OF LEMMA 4.1

The first part of Lemma 4.1 is intended only to be an intuitive aid, saying that “each collection of surfaces results from adding ends and handles to  $M_1$ ”. However, a rigorous proof is required for the statement that “the period problems arising from the additional ends are all solved by requiring  $\varepsilon = \text{length } A_i = \text{length } B_j$ ”.

For each surface, we always begin by choosing one-eighth of the original fundamental piece of the surface. This one-eighth piece is bounded by planar geodesics, and its conjugate surface is bounded by portions of lines. Before we consider any period problems, we must first establish existence of this conjugate surface, which then implies the existence of the original one-eighth piece (without solving for period problems yet).

The conjugate pieces exist because they are Jenkins–Serrin graphs. In all the cases we consider, they are Jenkins–Serrin graphs over a rectangle, and the boundary data is a finite constant over each of three sides of the boundary of the rectangle. On the fourth side, the boundary data alternates between  $+\infty$  and  $-\infty$  along adjacent intervals. The jump

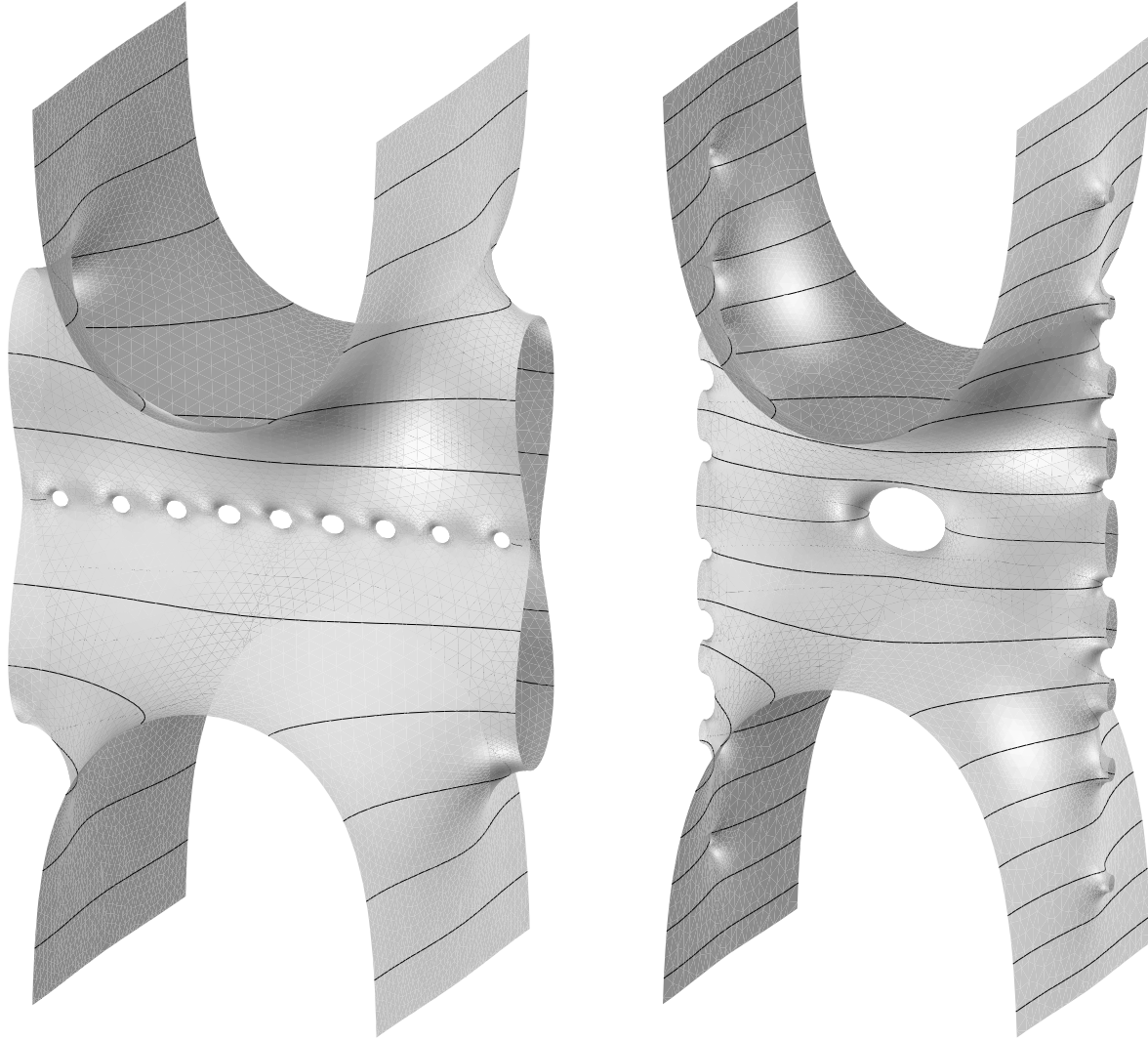


FIGURE 12. Fundamental pieces of  $M_1^{9+}$  (left) and  $M_1^{+,8-}$  (right).

discontinuities occur only at the corners of the rectangle and at points along the fourth side where the boundary data changes from  $+\infty$  to  $-\infty$ .

Recall Theorem 3.3. In our case, by applying a rigid motion and a homothety of  $\mathbb{R}^3$ , we may assume without loss of generality that

$$D = \{(x_1, x_2) \in \mathbb{R}^2 : 0 \leq x_1 \leq \delta, 0 \leq x_2 \leq 1\}$$

for some positive  $\delta$ , that there are three  $C_k$ 's which we define as

$$\begin{aligned} C_1 &= D \cap \{(x_1, 0) \in \mathbb{R}^2\}, \\ C_2 &= D \cap \{(\delta, x_2) \in \mathbb{R}^2\}, \\ C_3 &= D \cap \{(x_1, 1) \in \mathbb{R}^2\}, \end{aligned}$$

and that there are  $l$   $A_i$ 's and  $B_j$ 's, all of length  $\frac{1}{l}$  alternating along  $D \cap \{(0, x_2) \in \mathbb{R}^2\}$ . We have already incorporated the condition of Lemma 4.1, that is, that

$$\varepsilon = \text{length } A_i = \text{length } B_j = \frac{1}{l}.$$

Existence and uniqueness of a solution  $u$  to the minimal surface equation with the given boundary data now follows from Theorem 3.3. (The conditions on the polygons  $\mathcal{P}$  are trivially satisfied, since no such  $\mathcal{P}$  exists for the boundary conditions we are using.) Furthermore, the results in [Jenkins and Serin 1966] imply that  $u$  is finite at every point in the interior of  $D$ .

Let  $M$  denote the smallest closed minimal surface that contains the graph  $u$ . (Here we use the word “closed” in the sense that  $M$  contains all of its accumulation points.) Hence the interior of  $M$  is the interior of the graph  $u$ , and  $M$  contains its boundary  $\partial M$ , and the image of the vertical projection of  $M$  to the  $x_1x_2$ -plane is

$$D \setminus \{(0, x_2) \in \mathbb{R}^2 : x_2 \neq k/l \text{ some } k \in \mathbb{Z}\}.$$

We now prove Lemma 4.1 in a series of eight claims.

**Claim 1.**  *$M$  has finite total absolute curvature.*

*Proof.* As in the proof in [Jenkins and Serrin 1966, p. 334],  $u$  is the limit of a subsequence of minimal graphs  $\{u_n\}_{n=1}^\infty$  over  $\mathring{D}$ . The minimal graphs  $u_n$  are determined by replacing the boundary condition  $+\infty$  by  $+n$  on each  $A_i$ , replacing the boundary condition  $-\infty$  by  $-n$  on each  $B_j$ , and leaving the boundary data on  $C_1 \cup C_2 \cup C_3$  unchanged.

First we show that the total absolute curvature of the graph of  $u_n$  is bounded above by a finite bound independent of  $n$ , which follows easily from the Gauss–Bonnet formula. The boundary of  $u_n$  is polygonal with at most  $2l + 6$  boundary line segments, and at each intersection of adjacent boundary line segments the angle of intersection is  $\pi/2$ . Hence the total geodesic curvature of the boundary curve for the graph  $u_n$  is at most  $\frac{\pi}{2}(2l + 6)$ . The Gauss–Bonnet formula then implies

$$\int_{\text{Graph}(u_n)} |K| dA \leq \pi(l + 1) \tag{A-1}$$

for all  $n$ , where  $dA$  is the area form on  $\text{Graph}(u_n)$  induced by  $\mathbb{R}^3$ , and  $K$  is the intrinsic Gaussian curvature of  $\text{Graph}(u_n)$ .

Now we claim that for any compact convex domain  $D' \subset \mathring{D}$ , there exists a subsequence  $\{n_j\}_{j=1}^\infty$  such that the total absolute curvature of the graphs of  $u_{n_j}$  restricted to the domain  $D'$  converges to the total absolute curvature of the graph of  $u$  restricted to  $D'$ . That is, we claim that

$$\int_{\text{Graph}(u_{n_j}|_{D'})} |K| dA \rightarrow \int_{\text{Graph}(u|_{D'})} |K| dA \tag{A-2}$$

as  $n_j \rightarrow \infty$ . This follows from the fact that, as shown in [Jenkins and Serrin 1966],  $u_n|_{D'}$  converges uniformly to  $u|_{D'}$  as  $n \rightarrow \infty$ . The convergence (A-2)

is essentially known, and arguments showing it exist in several places. For example, a proof is contained in the arguments proving Theorem 2 in [Meeks and Yau 1982], which however are intended for more general ambient spaces; when the ambient space is  $\mathbb{R}^3$  the arguments can be considerably simplified. A simpler argument for the  $\mathbb{R}^3$  case can be found in [Courant 1950, Section III.2].

For completeness, in this paragraph we outline an argument showing (A-2). We know that the  $u_n$  converge uniformly to  $u$  over  $D'$ , by [Jenkins and Serrin 1966]. These graphs  $u_n|_{D'}$  (resp.  $u|_{D'}$ ) are graphs over convex domains in the  $x_1x_2$ -plane and hence are the unique compact minimal surfaces with respect to their boundaries. Hence they coincide as surfaces in  $\mathbb{R}^3$  with the Douglas–Rado solutions  $f_n : B^2 := \{(u, v) \in \mathbb{R}^2 : u^2 + v^2 \leq 1\} \rightarrow \mathbb{R}^3$  (resp.  $f : B^2 \rightarrow \mathbb{R}^3$ ) for their boundaries. That is, the surfaces  $f_n(B^2)$  and  $\{(x_1, x_2, u_n(x_1, x_2)) \in \mathbb{R}^3 : (x_1, x_2) \in D'\}$  (resp.  $f(B^2)$  and  $\{(x_1, x_2, u(x_1, x_2)) \in \mathbb{R}^3 : (x_1, x_2) \in D'\}$ ) coincide. The parametrizations  $f_n$  and  $f$  have the advantage that they are conformal, hence the coordinate functions  $f_n^i$  and  $f^i$ , for  $i = 1, 2, 3$ , are harmonic on  $B^2$ . Using arguments similar to those we use later to prove Claim 6 of this appendix, we can see that in fact

$$\frac{\partial u_n}{\partial x_1} \rightarrow \frac{\partial u}{\partial x_1}, \quad \frac{\partial u_n}{\partial x_2} \rightarrow \frac{\partial u}{\partial x_2}$$

converge uniformly over  $D'$  as well. (This is equivalent to showing that the normal vectors of the graphs converge uniformly over  $D'$ .) Once we know that first derivatives of  $u_n$  also converge uniformly, the arguments in the proof of Lemma 3.2 and the remark following it in [Courant 1950] can be applied: using the three-point condition as in [Courant 1950], we can find a subsequence  $f_{n_j}$  of the  $f_n$  which converge uniformly to  $f$  on  $\partial B^2$ . Since the functions  $f_{n_j}^i, f^i$  are harmonic, and hence the functions  $|f_{n_j}^i - f^i|$  always attain their maximums on  $\partial B^2$ , we conclude that  $f_{n_j} \rightarrow f$  uniformly on all of  $B^2$ . Uniform convergence for harmonic functions implies that the convergence is smooth (a basic property of harmonic functions; see [Gilbarg and Trudinger 1983, Theorem 2.10], for example). We conclude that the Douglas–Rado solutions  $f_{n_j}$  converge smoothly to  $f$ . Hence the total absolute curvature of the graphs

$u_{n_j}|_{D'}$  converges to the total absolute curvature of the graph  $u|_{D'}$ . This shows the convergence (A-2).

If the total absolute curvature of  $M$  is strictly greater than  $\pi(l+1)$ , then there exists some compact convex domain  $D' \subset \hat{D}$  such that the graph of  $u|_{D'}$  has total absolute curvature strictly greater than  $\pi(l+1)$ . However, then the convergence (A-2) contradicts equation (A-1). Therefore the total absolute curvature of  $M$  is at most  $\pi(l+1)$ , and Claim 1 is shown.  $\square$

**Claim 2.** *The are only a finite number of points of  $M$  at which the tangent plane is horizontal.*

*Proof.* The proof below is simply a modification of an argument in the proof of Theorem 3.1 of [Meeks and White 1991].

Consider the Gauss map

$$G : M \rightarrow S^2 = \{(x_1, x_2, x_3) \in \mathbb{R}^3 : x_1^2 + x_2^2 + x_3^2 = 1\}.$$

$M$  is the closure of the graph  $u$ , so  $M$  is orientable, and so  $G$  is well-defined. We can define  $G$  so that  $G(M) \subset S^2 \cap \{(x_1, x_2, x_3) \in \mathbb{R}^3 : x_3 \geq 0\}$ . With respect to conformal coordinates on  $M$ ,  $G$  is a holomorphic map from  $M$  to the upper hemisphere of  $S^2$ , hence  $G$  is a branched covering with boundary into the upper hemisphere. Furthermore, since  $\partial M$  consists of portions of lines parallel to the coordinate axes in  $\mathbb{R}^3$ ,

$$G(\partial M) \subset \{(x_1, x_2, x_3) \in S^2 : x_1 = 0 \text{ or } x_2 = 0 \text{ or } x_3 = 0\} \\ \cap \{(x_1, x_2, x_3) \in \mathbb{R}^3 : x_3 \geq 0\}.$$

Therefore the covering degree of  $G$  is a constant on each of the four sets

$$\{(x_1, x_2, x_3) \in S^2 : x_1 > 0, x_2 > 0, x_3 > 0\}, \\ \{(x_1, x_2, x_3) \in S^2 : x_1 < 0, x_2 > 0, x_3 > 0\}, \\ \{(x_1, x_2, x_3) \in S^2 : x_1 > 0, x_2 < 0, x_3 > 0\}, \\ \{(x_1, x_2, x_3) \in S^2 : x_1 < 0, x_2 < 0, x_3 > 0\}.$$

By Claim 1, these four constant covering degrees are all finite. If the inverse image  $G^{-1}(\vec{e}_3 = (0, 0, 1))$  were to contain infinitely many points of  $M$ , then at least one of these four constant covering degrees would not be finite. Hence  $G^{-1}(\vec{e}_3 = (0, 0, 1))$  is a finite set, showing Claim 2.  $\square$

Let  $P_s = \{(x_1, x_2, s) \in \mathbb{R}^3\}$  be the horizontal plane in  $\mathbb{R}^3$  of height  $s$ . An immediate corollary to Claim 2

is the following Claim 3. In Claim 3, by “nonsingular curves of  $\mathbb{R}^3$ ”, we mean curves of  $\mathbb{R}^3$  which are 1-dimensional submanifolds with boundary.

**Claim 3.** *There exists a constant  $L > 0$  such that, for all  $L' > L$ ,  $P_s \cap M$ ,  $s \in [L, L']$  (resp.  $s \in [-L', -L]$ ) is a smooth deformation (with respect to  $s$ ) from  $P_L \cap M$  to  $P_{L'} \cap M$  (resp. from  $P_{-L} \cap M$  to  $P_{-L'} \cap M$ ) through an embedded collection of nonsingular curves of  $\mathbb{R}^3$ .*

*Proof.* A singularity in this deformation can only occur at a point of  $M$  where the tangent plane is horizontal. By Claim 2, we can choose  $L$  large enough that no such horizontal points exist in  $\{(x_1, x_2, x_3) \in M : x_3 \geq L\}$  nor in  $\{(x_1, x_2, x_3) \in M : x_3 \leq -L\}$ . This proves Claim 3.  $\square$

Thus, by Claim 3, for any  $L' > L$ ,  $M \cap \{(x_1, x_2, x_3) \in \mathbb{R}^3 : x_3 \in [L, L']\}$  consists of a finite number of components, and each component is an embedded disk bounded by two vertical line segments, and one curve in  $P_{L'}$ , and one curve in  $P_L$ . We choose any component  $M_{\text{comp}}$  of  $M \cap \{(x_1, x_2, x_3) \in \mathbb{R}^3 : x_3 \in [L, L']\}$  and extend it by rotations of  $\pi$  radians about vertical boundary lines (this can be done, and the extended surfaces are smooth, by the Schwarz reflection principle, Theorem 3.1). Extending  $M_{\text{comp}}$  (and its extended surfaces) by these rotations a finite number of times results in a larger compact surface which still has only two vertical boundary line segments, and one boundary curve in  $P_{L'}$ , and one boundary curve in  $P_L$ . We make these rotational extensions enough times so that the distance in  $\mathbb{R}^3$  from any point in  $M_{\text{comp}}$  to the two boundary vertical line segments of the extended surface is greater than  $\frac{1}{4}(L' - L)$ . We call this extended surface  $M_{\text{comp}}^{\text{ext}}$ : it is an immersed compact disk in  $\mathbb{R}^3$ , and is not necessarily embedded. See Figure 13. (We will later see that  $M_{\text{comp}}^{\text{ext}}$  is indeed embedded for  $L$  large enough.)

**Claim 4.**  *$M_{\text{comp}}^{\text{ext}}$  is strongly stable.*

*Proof.* The image  $G(M_{\text{comp}})$  is contained in the upper hemisphere of  $S^2$  and does not contain the north pole  $\vec{e}_3$ . Since  $M_{\text{comp}}^{\text{ext}}$  is comprised of a finite number of pieces congruent to  $M_{\text{comp}}$  which are all images of vertical rotations of  $M_{\text{comp}}$ , it follows that  $G(M_{\text{comp}}^{\text{ext}})$  is also contained in the upper hemisphere and does

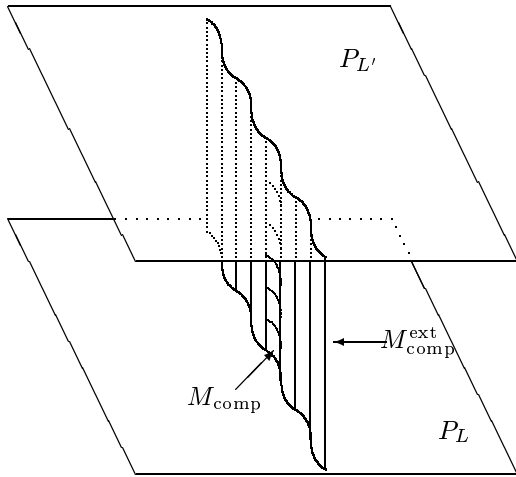


FIGURE 13. The construction of  $M_{\text{comp}}^{\text{ext}}$ .

not contain  $\vec{e}_3$ . In particular, the area of  $G(M_{\text{comp}}^{\text{ext}})$  in  $S^2$  is strictly less than  $2\pi$ .

Theorem 1.2 of [Barbosa and do Carmo 1976] tells us that if the area of  $G(M_{\text{comp}}^{\text{ext}})$  is less than  $2\pi$ , then  $M_{\text{comp}}^{\text{ext}}$  is stable. The map  $G$  is not required to be an injection in order for this theorem to hold, and the minimal surface need only be an immersion — it does not need to be an embedding. Furthermore, in [Barbosa and do Carmo 1976] the word *stable* is used in the strong sense; that is, a minimal surface is stable if the second derivative of area for any smooth nontrivial boundary-preserving variation is *strictly* positive. This shows Claim 4.  $\square$

For an oriented minimal surface  $\mathcal{M} \subset \mathbb{R}^3$  and sets  $A, B \subset \mathcal{M}$ , let  $\text{dist}_{\mathcal{M}}(A, B)$  be the intrinsic distance in  $\mathcal{M}$  between  $A$  and  $B$ . For each point  $q \in \mathcal{M}$ , let  $K_q$  be the Gaussian curvature of  $\mathcal{M}$  at  $q$ , and let  $\vec{N}_q$  be the oriented unit normal vector of  $\mathcal{M}$  at  $q$ . Let  $\vec{e}_1 = (1, 0, 0)$ , and let  $\langle \cdot, \cdot \rangle$  be the standard inner product on  $\mathbb{R}^3$ . Let  $\text{dist}_{\mathbb{R}^3}(A, B)$  be the distance in  $\mathbb{R}^3$  between two sets  $A, B \subset \mathbb{R}^3$ .

By Corollary 4 of [Schoen 1983] there exists a universal constant  $c$  such that

$$|K_q| < \frac{c}{\text{dist}_{\mathcal{M}}(q, \partial\mathcal{M})^2},$$

where  $\mathcal{M}$  is any compact stable minimal surface in  $\mathbb{R}^3$ , and  $q$  is any point in  $\mathcal{M}$ . This result (just like Theorem 1.2 of [Barbosa and do Carmo 1976]) does not require the surface  $\mathcal{M}$  to be embedded — only immersed. The constant  $c$  is universal in the sense that

it is independent of the choice of  $\mathcal{M}$ . (See Theorem 16.20 of [Gilbarg and Trudinger 1983] and Theorem 11.1 of [Osseman 1969] for related results.)

**Claim 5.** *On the surface  $\hat{M} := M_{\text{comp}} \cap \{(x_1, x_2, x_3) \in \mathbb{R}^3 : x_3 \in [\frac{1}{4}L' + \frac{3}{4}L, \frac{3}{4}L' + \frac{1}{4}L]\}$ , the Gaussian curvature  $K$  is uniformly bounded by*

$$|K| < \frac{16c}{(L' - L)^2}.$$

*Proof.*  $M_{\text{comp}}^{\text{ext}}$  is a compact minimal surface in  $\mathbb{R}^3$ , which is strongly stable by Claim 4. For all  $q \in \hat{M}$ ,  $\text{dist}_{M_{\text{comp}}^{\text{ext}}}(q, \partial M_{\text{comp}}^{\text{ext}}) \geq (L' - L)/4$ . Now we apply Corollary 4 of [Schoen 1983] and Claim 5 is proved. (See Figure 14.)  $\square$

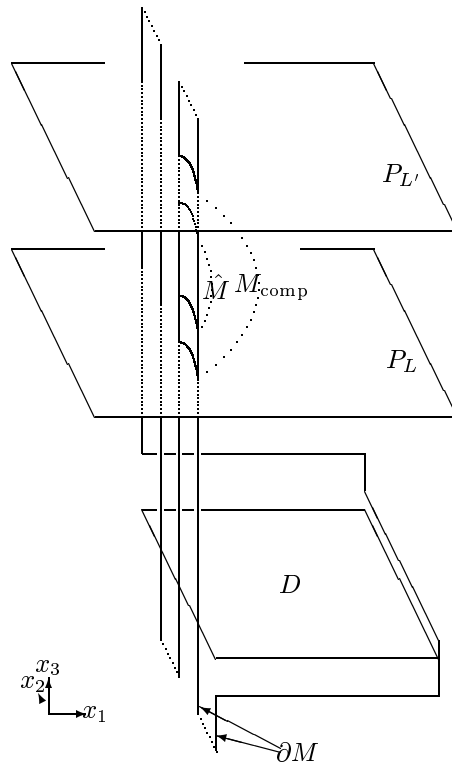


FIGURE 14. The location of  $\hat{M}$ , as defined in Claim 5.

Assume that  $L'$  is chosen large enough that

$$\frac{8\sqrt{c}\delta}{L' - L} < 1.$$

**Claim 6.** *At every point of  $M_{\text{comp}} \cap \{(x_1, x_2, x_3) \in \mathbb{R}^3 : x_3 \in [\frac{3}{8}L' + \frac{5}{8}L, \frac{5}{8}L' + \frac{3}{8}L]\}$ , we have*

$$|\langle \vec{N}, \vec{e}_1 \rangle| \geq \sqrt{1 - \frac{8\sqrt{c}\delta}{L' - L}}.$$

*Proof.* Suppose some point  $p \in M_{\text{comp}} \cap \{(x_1, x_2, x_3) \in \mathbb{R}^3 : x_3 \in [\frac{3}{8}L' + \frac{5}{8}L, \frac{5}{8}L' + \frac{3}{8}L]\}$  has normal  $\vec{N}_p$  so that

$$|\langle \vec{N}_p, \vec{e}_1 \rangle| < \sqrt{1 - \frac{8\sqrt{c}\delta}{L' - L}}.$$

Then there is a tangent vector  $\vec{T}$  at  $p$  such that  $\langle \vec{T}, \vec{e}_1 \rangle > \sqrt{\frac{8\sqrt{c}\delta}{L' - L}}$ . Assume  $L'$  and  $c$  are chosen large enough that  $L' - L > 1$  and  $c > 1024\delta^2$ . Consider a unit-speed geodesic  $\gamma(t) \subset \hat{M}$ ,  $t \in [0, (L' - L)/8]$  so that  $\gamma(0) = p$  and  $\gamma'(0) = \vec{T}$ , where the prime represents partial differentiation with respect to  $t$ . We define

$$t_0 := \sqrt{\frac{\delta(L' - L)}{2\sqrt{c}}}.$$

Since  $L' > L + 1$  and  $c > 1024\delta^2$ , we have that  $t_0 < (L' - L)/8$  and hence  $\gamma(t_0) \in \hat{M}$ . Let  $k_g(t)$  be the geodesic curvature of  $\gamma(t)$ . Since

$$|K_q| < \frac{16c}{(L' - L)^2}$$

for all  $q \in \hat{M}$  by Claim 5, and since  $\hat{M}$  is minimal, we have  $|k_g(t)| < 4\sqrt{c}/(L' - L)$  for all  $t \in [0, (L' - L)/8]$ . Thus  $|\gamma''(t)| < 4\sqrt{c}/(L' - L)$ . Writing  $\gamma(t) = (\gamma_1(t), \gamma_2(t), \gamma_3(t))$  in terms of coordinates in  $\mathbb{R}^3$ , we have  $|\gamma_1''(t)| < 4\sqrt{c}/(L' - L)$ . Then for  $t \in [0, (L' - L)/8]$ ,

$$\begin{aligned} |\gamma_1'(t) - \gamma_1'(0)| &= \left| \int_0^t \gamma_1''(s) ds \right| \\ &\leq \int_0^t |\gamma_1''(s)| ds < \frac{4\sqrt{c}}{L' - L} t, \end{aligned}$$

and thus  $\gamma_1'(t) > \gamma_1'(0) - (4\sqrt{c}/L' - L)t$ . Therefore

$$\begin{aligned} \gamma_1(t_0) &\geq \gamma_1(t_0) - \gamma_1(0) = \int_0^{t_0} \gamma_1'(t) dt \\ &> \int_0^{t_0} \left( \gamma_1'(0) - \frac{4\sqrt{c}}{L' - L} t \right) dt \\ &= \gamma_1'(0)t_0 - \frac{2\sqrt{c}}{L' - L} t_0^2 \\ &> \sqrt{\frac{8\sqrt{c}\delta}{L' - L}} t_0 - \frac{2\sqrt{c}}{L' - L} t_0^2 = \delta. \end{aligned}$$

The final inequality above follows from

$$\gamma_1'(0) = \langle \vec{T}, \vec{e}_1 \rangle > \sqrt{\frac{8\sqrt{c}\delta}{L' - L}},$$

and the final equality follows from the definition of  $t_0$ . This is a contradiction, since the vertical projection to the  $x_1x_2$ -plane of the geodesic  $\gamma(t) \subset \hat{M} \subset M$  is contained in  $D$ . This proves Claim 6.  $\square$

Now  $M_{\text{comp}}$  is one component of  $M \cap \{(x_1, x_2, x_3) \in \mathbb{R}^3 : x_3 \in [L, L']\}$  and thus  $M_{\text{comp}} = M_{\text{comp}}(L')$  depends on  $L'$ . We now wish to increase  $M_{\text{comp}}$  to a connected noncompact surface  $\tilde{M}$  that is independent of  $L'$ . Define

$$\tilde{M} := \bigcup_{L' > L} M_{\text{comp}}(L').$$

Thus  $M_{\text{comp}}(L') \subset \tilde{M}$  for all  $L'$ , and  $\tilde{M}$  is a disk bounded by one curve in  $P_L$  and by two upward-pointing vertical rays  $r_1, r_2$  with endpoints in  $P_L$ . (See Figure 15.) Since  $L' > L + \max(1, 8\sqrt{c}\delta)$  was arbitrary in the proof of Claim 6, an easy corollary of Claim 6 is the following:

**Claim 7.** *The normal vector  $\vec{N}$  on  $\tilde{M}$  converges to  $\pm\vec{e}_1$  at the end of  $\tilde{M}$ . More precisely, for all  $\rho \in (0, 1)$ , there exists  $\mathcal{L}(\rho) > 0$  such that at all points  $q \in \{(x_1, x_2, x_3) \in \tilde{M} : x_3 > \mathcal{L}(\rho)\}$ , the normal  $\vec{N}_q$  satisfies  $\|\vec{N}_q - \vec{e}_1\| < \rho$  or  $\|\vec{N}_q + \vec{e}_1\| < \rho$ .*

*Proof.* We choose  $s$  so that  $L' = 2s$ . By Claim 6, if  $L' > L + \max(1, 8\sqrt{c}\delta)$ , then

$$\langle \vec{N}_q, \vec{e}_1 \rangle^2 \geq 1 - \frac{8\sqrt{c}\delta}{2s - L}$$

for every point  $q \in P_s \cap M_{\text{comp}}$ . Define

$$\vec{N}_q^\perp := \vec{N}_q - \langle \vec{N}_q, \vec{e}_1 \rangle \vec{e}_1.$$

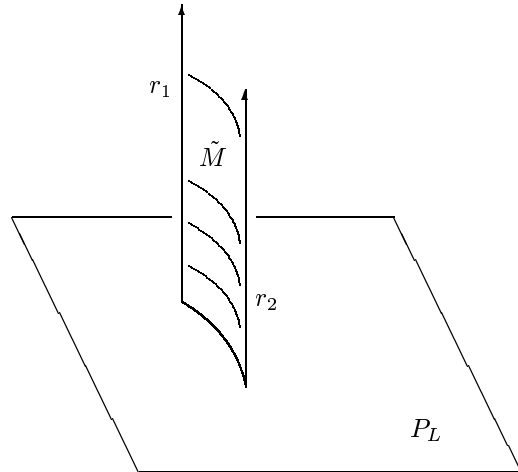


FIGURE 15. The surface  $\tilde{M}$ .

Then

$$\|\vec{N}_q^\perp\|^2 \leq \frac{8\sqrt{c\delta}}{2s-L}$$

and

$$\vec{N}_q \pm \vec{e}_1 = (\langle \vec{N}_q, \vec{e}_1 \rangle \pm 1)\vec{e}_1 + \vec{N}_q^\perp.$$

By a straightforward computation, choosing

$$s > \frac{16\sqrt{c\delta} + 3L}{3\rho^2} + 1$$

is sufficient to ensure

$$\min \|\vec{N}_q \pm \vec{e}_1\| < \rho \text{ and } L' > L + \max(1, 8\sqrt{c\delta}).$$

Claim 7 is shown.  $\square$

Using Claim 7 and elementary properties of conjugation, we now prove Lemma 4.1.

Note that  $\text{dist}_{\mathbb{R}^3}(r_1, r_2) = k/l$  for some positive integer  $k$ . By Claim 7 and the original construction of the boundary data (the choices we made for the  $A_i, B_j$ ) in the Jenkins–Serrin graph, we see that  $k = 1$ . Furthermore, by Claim 7, we have

$$\text{dist}_{\tilde{M}}(r_1, r_2) = \text{dist}_{\mathbb{R}^3}(r_1, r_2) = \frac{1}{l}. \tag{A-3}$$

Let  $\tilde{M}_{\text{conj}}$  be the conjugate surface of  $\tilde{M}$ . We have the following properties (see Figure 16):

1. Since conjugation is an isometry,  $\tilde{M}_{\text{conj}}$  is bounded by one smooth curve of finite length, and two smooth curves  $\hat{r}_1, \hat{r}_2$  of infinite length.
2. Since conjugation maps straight lines to planar geodesics,  $\hat{r}_1, \hat{r}_2$  are boundary planar geodesics of  $\tilde{M}_{\text{conj}}$  that are the images of the boundary rays  $r_1, r_2$ , respectively, under conjugation.

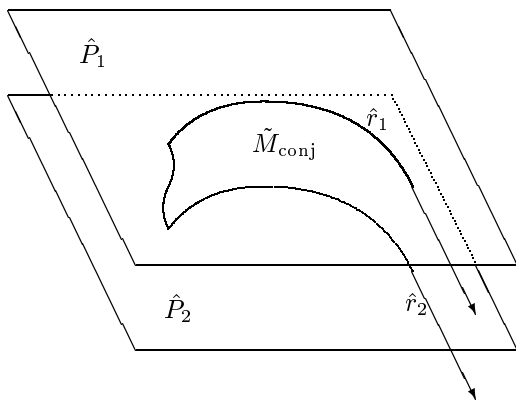


FIGURE 16. The conjugate surface of  $\tilde{M}$ .

3. Since conjugation preserves the Gauss map and hence also  $\vec{N}$ , the curves  $\hat{r}_1$  and  $\hat{r}_2$  each lie in a horizontal plane. We call these planes  $\hat{P}_1$  and  $\hat{P}_2$ .

4. Since the normal vector  $\vec{N}$  is preserved under conjugation,  $\vec{N}$  on  $\tilde{M}_{\text{conj}}$  converges to  $\pm\vec{e}_1$  at the end of  $\tilde{M}_{\text{conj}}$ .

5. By property 4 above,

$$\text{dist}_{\mathbb{R}^3}(\hat{P}_1, \hat{P}_2) = \text{dist}_{\tilde{M}_{\text{conj}}}(\hat{r}_1, \hat{r}_2).$$

6. Since conjugation is an isometry,

$$\text{dist}_{\tilde{M}_{\text{conj}}}(\hat{r}_1, \hat{r}_2) = \text{dist}_{\tilde{M}}(r_1, r_2).$$

Finally, from equation (A-3) and properties 5 and 6 above, we conclude:

**Claim 8.**  $\text{dist}_{\mathbb{R}^3}(\hat{P}_1, \hat{P}_2) = \frac{1}{l}.$

On the conjugate  $\tilde{M}_{\text{conj}}$  of  $\tilde{M} \subset \{(x_1, x_2, x_3) \in M : x_3 \geq L\}$ , the period problem at the end is a vertical translation comprised of one reflection through  $\hat{P}_1$  composed with one reflection through  $\hat{P}_2$ . Thus the period problem is a vertical translation of length exactly  $\frac{2}{l}$ , by Claim 8. Likewise, the same holds for the conjugate surface of any other components of  $\{(x_1, x_2, x_3) \in M : x_3 \geq L\}$  and any components of  $\{(x_1, x_2, x_3) \in M : x_3 \leq -L\}$  as well, when  $L$  is chosen large enough. Since the boundary behavior alternates between  $+\infty$  and  $-\infty$  along the alternating  $A_i$ 's and  $B_j$ 's, the normal vector of the graph  $u$  must alternately approach  $+\vec{e}_1$  and  $-\vec{e}_1$  along the  $A_i$ 's and  $B_j$ 's. Therefore, as one travels along the line segment  $D \cap \{(0, x_2) \in \mathbb{R}^2\}$ , the vertical direction of the translation periods at the ends of the conjugate surface of  $M$  alternates between upward and downward translations of length  $\frac{2}{l}$ .

Thus Lemma 4.1 is shown.

**ACKNOWLEDGEMENTS**

The computer graphics in the figures were created using the MESH software produced by James T. Hoffman of the Mathematical Sciences Research Institute, Berkeley, California, USA.

**REFERENCES**

[Barbosa and do Carmo 1976] J. L. Barbosa and M. do Carmo, "On the size of a stable minimal surface in  $R^3$ ", *Amer. J. Math.* **98**:2 (1976), 515–528.

- [Courant 1950] R. Courant, *Dirichlet's principle, conformal mapping, and minimal surfaces*, Interscience, New York, 1950. Reprinted by Springer, New York, 1977.
- [Dierkes et al. 1992] U. Dierkes, S. Hildebrandt, A. Küster, and O. Wohlrab, *Minimal surfaces, I: Boundary value problems*, Springer, Berlin, 1992.
- [Gilbarg and Trudinger 1983] D. Gilbarg and N. S. Trudinger, *Elliptic partial differential equations of second order*, Second ed., Grundlehren der Mathematischen Wissenschaften **224**, Springer, Berlin, 1983. Revised third printing, 1998.
- [Jenkins and Serrin 1966] H. Jenkins and J. Serrin, "Variational problems of minimal surface type, II: Boundary value problems for the minimal surface equation", *Arch. Rational Mech. Anal.* **21** (1966), 321–342.
- [Karcher 1991] H. Karcher, "Construction of higher genus embedded minimal surfaces", pp. 174–191 in *Geometry and topology of submanifolds, III* (Leeds, 1990), edited by L. Verstraelen and A. West, World Sci. Publishing, River Edge, NJ, 1991.
- [Karcher and Polthier 1993] H. Karcher and K. Polthier, 1993. Personal communications.
- [Meeks and Rosenberg 1990] W. H. Meeks and H. Rosenberg, "The maximum principle at infinity for minimal surfaces in flat three manifolds", *Comment. Math. Helv.* **65**:2 (1990), 255–270.
- [Meeks and White 1991] W. H. Meeks and B. White, "Minimal surfaces bounded by convex curves in parallel planes", *Comment. Math. Helv.* **66**:2 (1991), 263–278.
- [Meeks and Yau 1982] W. H. Meeks and S. T. Yau, "The classical Plateau problem and the topology of three-dimensional manifolds. The embedding of the solution given by Douglas–Morrey and an analytic proof of Dehn's lemma", *Topology* **21**:4 (1982), 409–442.
- [Osserman 1969] R. Osserman, *A survey of minimal surfaces*, Van Nostrand Reinhold Co., New York, 1969. Reprinted by Dover, New York, 1969, 1986.
- [Schoen 1983] R. Schoen, "Estimates for stable minimal surfaces in three-dimensional manifolds", pp. 111–126 in *Seminar on minimal submanifolds*, edited by E. Bombieri, Annals of Math. Stud. **103**, Princeton Univ. Press, Princeton, 1983.
- [Wei 1992] F. S. Wei, "Some existence and uniqueness theorems for doubly periodic minimal surfaces", *Invent. Math.* **109**:1 (1992), 113–136.
- [Wohlgemuth 1997] M. Wohlgemuth, "Minimal surfaces of higher genus with finite total curvature", *Arch. Rational Mech. Anal.* **137**:1 (1997), 1–25.

Wayne Rossman, Faculty of Science, Kobe University, Kobe 657-8501, Japan (wayne@math.kobe-u.ac.jp, <http://www.math.kobe-u.ac.jp/HOME/wayne/wayne.html>)

Edward C. Thayer, ZymoGenetics Inc., 1201 Eastlake Ave East, Seattle WA, 98102, United States (thayer@zgi.com)

Meinhard Wohlgemuth, Mathematisches Institut, Universität Bonn, Beringstraße 1, 53115 Bonn, Germany (meinhard@math.uni-bonn.de)

Received May 26, 1998; accepted in revised form May 6, 1999